AD-A181 313 A REVIEW OF AUSTRALIAN INVESTIGATIONS ON AERONAUTICAL FATIGUE DURING THE..(U) AERONAUTICAL RESEARCH LABS MELBOURNE (AUSTRALIA) G S JOST APR 87 ARL-STRUC-TM-457 1/1

UNCLASSIFIED F/G 20/11 NL

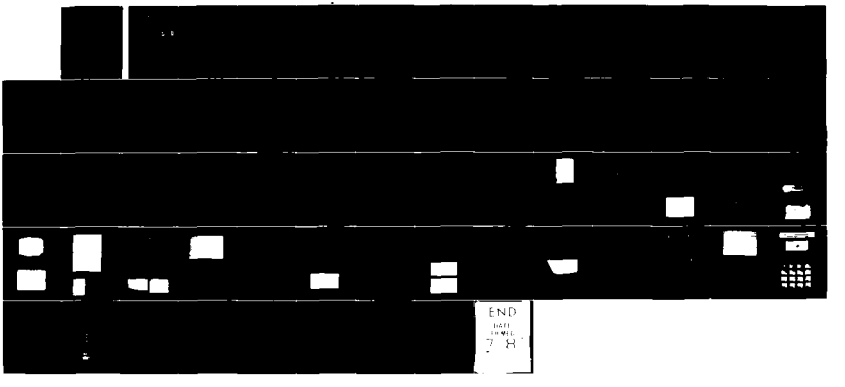

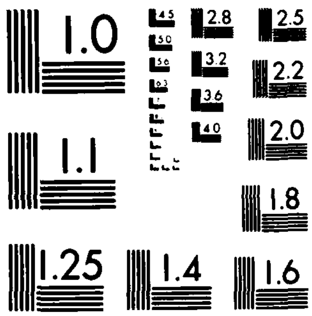

MICROCOPY RESOLUTION TEST CHART
NATIONAL BUREAU OF STANDARDS-1963-A

UNCLASSIFIED

(12)

ARL-STRUC-TM-457

AR-004-521

DEPARTMENT OF DEFENCE

DEFENCE SCIENCE AND TECHNOLOGY ORGANISATION

AERONAUTICAL RESEARCH LABORATORIES

MELBOURNE, VICTORIA

Structures Technical Memorandum 457

A REVIEW OF AUSTRALIAN INVESTIGATIONS ON AERONAUTICAL FATIGUE DURING THE PERIOD APRIL 1985 TO MARCH 1987

Edited by

G.S. JOST

APRIL 1987

UNCLASSIFIED

87

AR-004-521

DEPARTMENT OF DEFENCE
DEFENCE SCIENCE AND TECHNOLOGY ORGANISATION
AERONAUTICAL RESEARCH LABORATORIES

Structures Technical Memorandum 457

A REVIEW OF AUSTRALIAN INVESTIGATIONS ON AERONAUTICAL FATIGUE DURING THE PERIOD APRIL 1985 TO MARCH 1987

Edited by

G.S. JOST

SUMMARY

This document was prepared for presentation to the 20th Conference of the International Committee on Aeronautical Fatigue scheduled to be held in Ottawa, Canada, on June 8 and 9, 1987.

A review is given of the aircraft fatigue research and associated activities which form part of the programmes of the Aeronautical Research Laboratories, Universities, the Department of Aviation and the Australian aircraft industry. The major topics discussed include the fatigue of both civil and military aircraft structures, fatigue damage detection, analysis and repair and fatigue life monitoring and assessment.

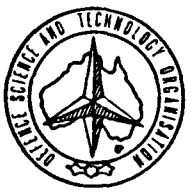

POSTAL ADDRESS: Director, Aeronautical Research Laboratories,
P.O. Box 4331, Melbourne, Victoria, 3001, Australia.

CONTENTS

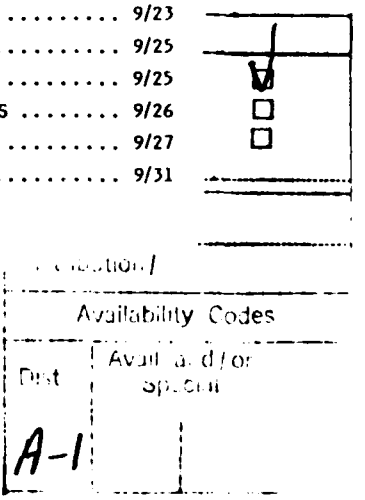

9.1 INTRODUCTION

This Review of Australian investigations on aeronautical fatigue in the 1985 to 1987 biennium has been made possible by the co-operation of the author's colleagues at the Aeronautical Research Laboratories, Universities, the Department of Aviation and in the Australian aircraft industry, and their contributions to this Review are gratefully acknowledged. Further information on any item may be obtained from the contacts given. The names, addresses and abbreviations of contributing organisations are as follows :

ARL	Aeronautical Research Laboratories, GPO Box 4331, Melbourne, Victoria, 3001.
DOA	Department of Aviation, PO Box 367, Canberra, ACT, 2601.
GAF	Government Aircraft Factories, PO Box 4, Port Melbourne, Victoria, 3207.
HDHV	Hawker de Havilland (Victoria) Pty Ltd, GPO Box 779H, Melbourne, Victoria, 3001.
UOM	University of Melbourne, Parkville, Victoria, 3052.
UOS	University of Sydney, New South Wales, 2006.

9.2 FATIGUE OF MILITARY AIRCRAFT STRUCTURES

9.2.1 Mirage IIIO (J.M. Grandage - ARL)

The previous Australian ICAF review /1/ referred to damage tolerance assessment work on the RAAF Mirage fleet. Since that time strain data from flight tests and ground calibrations have been analysed and this has led to the conclusion that structural control points in the rear fuselage and front fuselage are not stressed sufficiently highly to require detailed damage tolerance assessment. The Swiss fatigue test has been completed with the exception of the teardown inspection of some parts of the airframe. These include the fin which is thought to contain a crack at the main spar root.

Crack growth calculations for damage tolerance assessment have been concerned with control points in the wing and fuselage frame 26. The Wheeler crack growth model has been successfully validated against crack growth data from ARL tests on component simulation specimens, and also against data from cracks generated in the wing during the Swiss fatigue test. However attempts to validate the model against Swiss crack growth data from frame 26 were unsuccessful. Predicted crack growth rates from the model (using the best estimate of local strain response based on existing information) were much slower than those measured on test. For this reason the inspection intervals calculated by the model for frame 26 need careful interpretation. This is under consideration at present.

References /2/, /3/ and /4/ discuss work carried out on this project in detail.

9.2.2 CT4-A Air Trainer (J.M. Grandage - ARL)

ARL has carried out a fatigue test on the CT4A aircraft, some aspects of which were summarised in the previous review. The test achieved failures at almost identical locations in the port and starboard wings, as well as a failure in the centre section joint close to the aircraft centre-line. Failure times were 51,141 hours (port wing), 55,380 hours (centre joint) and 60,700 hours (starboard wing). The test as a whole is reported in /5/, while /6/ and /7/ discuss the test load sequences and the flight trials programme.

Service life estimates for the RAAF fleet have been based on this test, recognising that for the later phase of the test the loading was more severe than the service load spectrum (see /1/, /5/). The main characteristic of this more severe load spectrum was that many of the lower load magnitudes which had been applied in the earlier part of the test were eliminated. Using the conventional relative Miner approach for interpreting the test life in terms of the service load spectrum, it was estimated from cumulative damage calculations that the centre joint would fail in service before the wing failure location. Different fatigue data are appropriate to the two failure locations, with the data for the centre joint predicting proportionally more damage from low loads than for the wing. The lower relative frequency of low loads in the second phase of the test resulted in the centre joint experiencing a lower damage rate than the wing. In other words, the enhanced load sequence applied late in the test may have encouraged failures to occur in the reverse order from that which would be expected in service. This more severe load spectrum was introduced when financial constraints required the test to be completed within limited calendar time.

9.2.3 GAF Nomad (L.T. Tuller - GAF)

Progress on the Nomad full-scale fatigue test has been reported regularly in past ICAF Reviews. A comprehensive recent account is given in /8/. To the end of February 1987 a total of 196,000 flight hours have been achieved.

The major event during the past biennium has been the totally unexpected failure of the second stub-wing front spar from a hole near the strut pick-up fitting at a life much lower than the first, /1/. The first failure at this location occurred at 138,000 flights. The stub-wing was then rebuilt with a new front spar, retaining as much of the original structure as possible. In view of the very satisfactory life achieved by the first spar, the second was not expected to fail within the period of this Review.

The second stub-wing failed in the same starboard location as the first after only 37,000 flights, Fig.9.1. Cracking was underway at the same location on the port side, and at several adjacent rivet holes. Since this life was only one quarter of the original, the failure became an immediate safety issue for service Nomad aircraft. All aircraft beyond 3,000 hours are being inspected in this region. Some 20 aircraft in several countries have been inspected, and no cracking has been found. Inspectors did report, however, such items as scores, problems at the skin/spar interface, hole elongation in the skin, loose rivets, fretting and low edge margins.

Fractographic analysis of the second spar failure, and comparison with the first, shows that the (deduced) life to crack initiation of the second failure was only about one-fifth that of the first failure, Fig. 9.2. The crack growth rates through the spar flanges for both failures were similar, but crack growth in the spar cap of the second spar was much more rapid. Although investigations to date have not revealed positively the reasons for these differences, it is noted that service stub-wing front spars were manufactured from bar, plate or extruded stock: in the case of the test article the first spar was machined from plate, the second from extrusion. Overall, the main reason for the four-fold difference in lives corresponds to the difference in crack initiation times.

The short life of the second stub-wing front spar has given rise to consideration of fatigue life enhancement of the critical region. There are at least two major concerns in this case. First, the problem of short hole edge margins : the field inspection revealed some aircraft with edge margins of the order of 1.0. With holes so close to the edge, a process such as cold-expansion needs to be well proven before its adoption in service. Secondly, many Nomad aircraft operate in a marine environment, and the possibility of stress corrosion cracking (at the free edge) needs to be checked. An appropriate programme to investigate these aspects is underway.

In anticipation of a satisfactory outcome from the above investigations, the second rebuild of the test article stub-wing (including the third front spar) has included extensive use of the FTI cold-expansion process in the fatigue-critical regions in 89 holes. Testing began again in August 1986 and by the end of January had accumulated 17,000 flights. By the end of 1987 the new structure will have seen 50,000 flights and original structure 225,000 flights. If the structure is still intact at that stage, the level of loading will be increased, with the aim of forcing failure of the main wing.

Although the total number of identified crack sites to date is 234, the great majority of these are in the 'nuisance' category. Significant cracking has now occurred in the second wing-strut upper fitting (the first failed at 78,000 hours) and all lower wing skin stringers near station 210 have failed. Wing rib cracking at station 114 was reported in the previous Review /1/. The test is continuing to provide an ideal opportunity for developing and evaluating repair schemes and inspection techniques.

9.3 FATIGUE IN CIVIL AIRCRAFT (R.B. Douglas - DOA)

9.3.1 Boeing 747 Forward Fuselage Cracking

The continuing airworthiness of Boeing 747 aircraft has been a major focus of attention over the past two years. The most significant and far-reaching problem concerns the discovery of substantial cracking in the forward fuselage structure, commonly known as Section 41 (S41).

Detailed inspections by one operator on several high time 747 aircraft in late 1985 identified a large number of fatigue cracks in the forward fuselage, Fig 9.3. As a result of these inspections, additional high time aircraft were inspected to ascertain the extent of possible fleetwide cracking. One aircraft was found to have eleven frames cracked, three adjacent frames of which were completely severed. The fail-safe capabilities of the aircraft were affected by the extent of cracking being observed.

In early February 1986 the US FAA issued an urgent Airworthiness Directive calling for external skin inspections around known problem areas for aircraft which had achieved more than 10,000 flights. The Department of Aviation followed with an equivalent directive, on the basis that the current inspection schedule was clearly not adequate to assure continued airworthiness of the aircraft. The skin inspections were an interim measure based on residual strength analysis of fuselage structure with adjacent frame segments severed. No skin cracking was found on the five affected Qantas aircraft, nor were any reported from other overseas operators.

Boeing subsequently developed internal visual inspection procedures for the fuselage frames, which were made mandatory by the Department. Inspections were divided into "phase 1" which cover the local area where the worst cracking has been found, and "phase 2" which covered a major portion of the forward fuselage. The threshold for both inspections was 10,000 flight cycles. At the time the FAA decided to only make the phase 1 inspections mandatory, and issued a Notice of Proposed Rulemaking for phase 2 inspections. These inspections placed a considerable maintenance cost burden on the operators.

Several Qantas and ex-Qantas aircraft were inspected to the phase 1 and 2 requirements. Serious damage was discovered in the Qantas aircraft undergoing phase 1 inspections, with four cases reported where two adjacent frames were found cracked on aircraft with around 10,500 flight cycles. In one case an aircraft with 10,025 flight cycles contained a 380 mm frame web crack. Significant cracking was also being discovered in other separate structural items in S41.

Based on the Qantas inspection results the Department became concerned about the adequacy of the 10,000 cycle threshold, and consulted with Qantas on adopting a lower inspection threshold. Of the 140 aircraft inspected world wide in accordance with phase 1 and 2 requirements by late March 1986, there were seven instances of two adjacent frames severed, three of which were discovered on Qantas aircraft. There were also twenty seven cases of one frame severed.

Boeing and the FAA subsequently developed a revised S41 inspection program where the threshold for certain areas was dropped to 8000 flight cycles. The total area inspected at 10,000 flight cycles was reduced, but in three further steps of 3000 flight cycle intervals the area is gradually increased, until at 19,000 flight cycles all of S41 is inspected.

The proposed multi-phased inspections were made mandatory by the Department, and included several changes. The initial threshold was dropped to 7000 cycles and, based on local experience, the areas being inspected were extended. As of early December 1986, three Qantas aircraft had completed the 7000 cycle inspection resulting in the discovery of a 46 mm frame web crack. Two aircraft have also completed the 10,000 cycle inspection resulting in fourteen frame cracks being discovered, with one crack extending 20 mm. Table 9.1 summarises the occurrence of severed frames in section 41 of Qantas aircraft. There have been numerous reports of cracked frames in other 747 aircraft.

The Department has been trying to explain the apparent seriousness of cracking experienced in Qantas aircraft compared to the world fleet. Cracked frame segments were examined in the Department's Materials Evaluation Facility. More than one mode of failure was observed, and it appeared that cracks may have propagated by both fatigue and/or stress corrosion. It was postulated that the longer flight-stage segments of Qantas aircraft combined with stress corrosion might explain the extensive cracking. Boeing have since confirmed that their investigations indicate only fatigue (pressurisation) related cracking in S41. A more likely, although still inconclusive, explanation for the seriousness of cracking in Qantas aircraft might be inconsistencies between airline inspection procedures.

The discovery of extensive fleetwide cracking raises questions regarding the effectiveness of the Supplemental Structural Inspection Program (SSIP) to detect cracking in the 747 fleet. Of the 118 SSIP candidate aeroplanes, 93 have reported cracks, including major damage. Although the above data undermines the apparent effectiveness of the SSIP, the fact that the program was delayed in its introduction, along with a one year compliance time, appear to have

decreased the SSIP effectiveness for S41 cracking. It is likely that had the program been implemented sooner, the problem would have been identified earlier.

The length of frame web cracks for S41 show a very low correlation with time (flights) in service. The fact that crack data were obtained from inspections conducted at relatively short notice, as opposed to planned inspections over the life of the aircraft, could explain this. Several major cracks on Qantas aircraft showed the largest crack length per unit time in service yet reported.

The discovery of multiple fractured adjacent frames, with no associated skin cracking, raises questions regarding the adequacy of current damage tolerance requirements. It is doubtful whether current fuselage structure with multiple adjacent frames severed would sustain a one bay (20 inch) skin crack under regulatory fail-safe loads. Multiple site damage continues to be a major problem in damage tolerance substantiations, with the recent 747 service cracking only highlighting the need for a review on this subject.

9.3.2 Fokker F28 Rear Pressure Bulkhead Cracking

Several reported incidents of severe cracking in the rear pressure bulkhead webs of Fokker F28 aircraft, including one case which resulted in an in-flight depressurisation, have caused some concern over the adequacy of the current inspection procedures called up by the manufacturer's Structural Integrity Program (SIP).

The F28 has a flat rear pressure bulkhead stiffened by vertical and horizontal beam members on its rear face, Fig. 9.4. The SIP relies on visual inspection from the rear face of the bulkhead to detect beam flange and bulkhead web cracking which result from local deflections due to pressurisation loads. Web cracking has been reported between the two rows at rivets connecting the horizontal support beams to the web, Fig. 9.5. This type of web crack is hidden by the beam when viewed from the rear face of the bulkhead, as specified in the SIP. The underlying principle behind the visual bulkhead inspection technique is that beam flange cracking and/or nicotine stains would be indicators of web cracking. In addition, since the web crack occurs between the two rivet rows, the parts of the bulkhead web remain attached to each other via the horizontal support beams thereby reducing the risk of explosive decompression. Web cracks extending beyond the SIP quoted critical crack length of 800 mm should be stopped by the vertical reinforcement beams.

Two separate incidents have cast doubt on the suitability of the web inspection procedure. The aircraft involved in the in-flight decompression suffered an uncontained fatigue failure of the rear pressure bulkhead web. Inspections were being conducted in accordance with the SIP every 3300 flights. The last bulkhead inspection was conducted 2000 flights before failure, at which time neither web nor beam flange cracking was evident. The crack extended just below the lower rivet holes of horizontal beam VIII, not between the beam rivet lines. A section of the failed bulkhead is shown in Fig. 9.6. Another large crack was evident along the lower row of rivets at beam VI.

The Department's Materials Evaluation Facility examined the failed section, and determined that fatigue initiated from multiple origins on the forward surface of the web. A series of cracks propagated transversly through the web, and then longitudinally, subsequently joining with other fatigue cracks leading eventually to an overload failure.

Striation counting indicated that one fatigue crack propagated from initiation to penetration of the rear face of the web in 3800 cycles (flights). Because the overall fatigue cracking propagated from many origins and each origin initiated at a different time, it was not possible to ascertain the total cycles from the first initiation of a crack to failure of the web. However, it would appear that fatigue cracks had been present in the web for more than 3,800 flights.

Another complicating feature of this failure is the presence of a factory-installed doubler on the front face of the bulkhead, as shown in Fig. 9.7. The doubler was installed at manufacture to rectify surface damage. The laboratory analysis revealed the presence of doubler sealant material on the fracture surface, indicating that the crack was present whilst the sealant was still fluid. The sealant indication could only occur if the sealant around the edge of the doubler had not completely set and hardened prior to cracking, in which case migration of sealant into a through-crack would be possible. This is also supported by the fact that the fracture surface at this location was the most heavily

oxidised and stained and appeared to be the first area of cracking to initiate. At the very least, the presence of sealant indicates early crack initiation and subsequent through-cracking.

The doubler installed by the manufacturer should have extended at least two rivet rows below the rivet line row attaching horizontal beam VIII (Fig. 9.7), as specified in the Structural Repair Manual. This would have produced a gradual stiffness change, as opposed to the sudden change indicated by Fig. 9.7. Whether the presence of the doubler as installed initiated the cracking is still an open question, especially considering the presence of sealant material on the fracture surface.

The current inspection procedures were further cast into doubt by the discovery of a 530mm web crack during a major inspection. The crack was located under horizontal beam X (Fig. 9.4) between BL425L and BL1050L. The Department is currently consulting with the manufacturer on changing the SIP inspection procedures to incorporate an NDI technique for web cracking. The current visual inspection method is clearly inadequate unless inspections are extended to the front face of the web in addition to the rear face.

Fatigue damage initiating at multiple sites was positively identified as the cause of web failure. As in the case of Boeing 747 cracking reported in Section 9.3.1, this incident demonstrates the need for a reconsideration of multiple site damage and its implication on the damage tolerance assessment of major airframe components.

9.3.3 Gulfstream (Rockwell) 112/114 Main Spar Cracking

In the 1983-1985 Australian Review, /1/, early and completely unanticipated fatigue problems were reported in the wing spars of the Partenavia P68. A similar problem has now occurred with the American designed and manufactured Rockwell (now Gulfstream) 112 and 114 model aircraft /9/.

A high proportion of the Australian fleet of these aircraft has experienced cracking in the upper cap of the main wing spar, Fig. 9.8. Cracks of up to 36 mm long have been found, running spanwise in the vertical leg of the extruded T-section. This type of cracking will reduce the compressive stability of the spar cap, thereby increasing the risk of wing collapse under severe positive g manoeuvres or upgusts.

The cracking is caused by poor detail design in the method of attachment of the main landing gear mechanism. The landing gear side-brace bracket is cantilevered forward from the spar, Fig. 9.9, causing the inboard-outboard loads being reacted by the side-brace fitting during landing gear extension and retraction to produce out-of-plane bending stresses in the spar. These stresses have proved to be sufficiently high to produce cracking in some aircraft before they reach 500 hours time in service. The manufacturer's original fatigue life evaluation for the wing, by analysis only, predicted a safe life of 11,200 hours.

The manufacturer has developed a repair and preventative modification for this problem, Fig. 9.10. The cost to owners is substantial, and the American owner's group is now taking legal action against the manufacturer.

This case highlights the dangers inherent in the short-cut analytical fatigue evaluations which are common for this class of aircraft. Too often they produce results which are grossly inaccurate because secondary loading sources and/or stress concentrating details have not been accounted for in the analysis. A proper fatigue evaluation, including a fatigue test, may have detected this problem earlier, enabling design changes to be made to production aircraft.

9.3.4 Grumman G-164A Ag Cat

A failure has been experienced in the port aileron-interconnect strut of a Grumman G-164A cropdusting aircraft. A crack propagated chordwise and allowed the strut to flex excessively in flight; this was observed by the pilot. Final failure occurred after landing, probably during removal. The failure occurred one third of the way from the upper end. The starboard strut was inspected and no fault found.

At the date of the incident, this aircraft had flown 5,544 hours since new. The operating time on the strut has not been determined. A review of US and Australian defect report registers suggests that this is the first reported failure of this potentially catastrophic type.

Metallurgical examination /10/ shows that the crack initiated at a corrosion pit located in the bottom of an impact damage mark - probably a stone chip. The total depth of this stress raising damage was approximately 0.27 mm. The crack is thought to have propagated from initiation to 88 percent of the section area in about 80,000 load cycles. Corroded areas found on the fracture surface indicate that a crack extending to the surface had existed for some time, probably weeks, before the incident.

It is not clear whether the circumstances which caused the crack to initiate at about 5500 hours are unique to that aircraft or whether, alternatively, the failure is a forerunner of other cracks around a 5500 hour mean time to failure. The most disconcerting aspect of this incident is that the crack was able to propagate undetected to such an extent. The crack propagation rate, or implied detection difficulty, can be expected to be common to all G-164 aircraft.

While the identifiable loads on the strut are comparatively small and infrequent, it seems clear that some additional loads are being applied inadvertently, probably at high frequency. The sources of these loads are not definitely known but aileron buffet in steep turns, and torsional flexural flutter of the strut itself, are possible suspects. Fluttering or 'buzzing' is said to be common and associated with struts having worn end fittings. Additional stresses may be caused by misaligned end fittings.

With such uncertainty, it is impossible to predict a likely fatigue life for these struts. The one known failure occurred in circumstances which are not quantifiable and which may well be atypical. Accordingly, it would not be reasonable at this stage to impose a mandatory replacement life for these struts.

9.3.5 Sailplane Fatigue Investigation

The Department of Aviation, in conjunction with the Gliding Federation of Australia, is sponsoring a full-scale fatigue test of a Schemp-Hirth Janus-B glider, to be conducted by the Royal Melbourne Institute of Technology. Progress reports on this project have featured in past ICAF reviews.

A substantial amount of work has been completed on the project. The test rig has been commissioned following the installation of some 300 strain gauges on the test article. A flight-by-flight test load sequence, which was derived from an exhaustive flight strain survey covering typical glider operations within Australia, is nearing final definition.

The Australian program has been firmly oriented towards failure modes and failure detection aspects. Future progress is dependent primarily on funding, and the objectives could also be subject to review depending on the objectives and results of other (overseas) investigations.

9.3.6 Bell 205 Main Rotor Blade Cracking

Following the onset of a rapidly increasing once-per-revolution lateral in-flight vibration, a large chordwise crack was found in the underside of one main rotor blade, near the root, in an Australian registered helicopter. The crack emanated from under the steel grip pad and extended through the grip plate and doublers, running towards the leading and trailing edges, into the skin, for a total length of about 250 mm, Fig. 9.12.

When the blade was sectioned for laboratory investigation, it was found that, in addition to the crack, the steel grip pad had become disbonded from the blade over about 75% of the bond area. The appearance of the disbond area suggested that it was of long standing.

The blade crack, which was confirmed as having propagated by fatigue /11/, had initiated in the lower surface grip plate (adjacent to the steel pad), on both forward and rearward sides of the retention pin hole. There were no stress raisers (corrosion pits, nicks, scratches, etc.) associated with initiation of the crack, although there was some surface corrosion present in the bore of the hole and on the fracture surface. Cracking propagated for 200 mm towards the trailing edge through the grip plate, doubler stack and skin, and through the rear wall of the D-spar. Crack growth towards the leading edge propagated for 50 mm through the grip plate and doubler stack, the abrasion strip and the lower part of the D-spar. The nose block was not cracked.

It is postulated that the grip plate bond separation occurred first. The resulting loss of load transfer from the aluminium alloy grip plate to the steel grip pad and thence to the retention pin bush, increased the direct load transfer from the aluminium alloy plate to the bush, thus leading to the initiation of the fatigue crack in the plate.

The blade total time in service was 2200 hours. Records showed that, in addition to the required daily inspections, it had been inspected each 1000 hours/12 months in accordance with SB 205-75-5C. The last inspection was carried out 1 '0 hours prior to crack detection. Fractographic examination indicates that the fatigue crack had grown over a period of about 250 flights. This suggests that the visual inspections for bond line separation may be inadequate and this question has been raised with the manufacturer. Pending their investigation and advice, the particular helicopter operator concerned is sponsoring research work to develop an NDI technique to inspect the bond line.

In the meantime, Australian operators of both Bell 204/205 and Bell 212 helicopters have been reminded to exercise vigilance when carrying out the visual inspection. The area must be kept clean to facilitate the visual inspection, and the use of a magnifying glass is suggested.

9.3.7 Bell 47 Main Rotor Grip Failure

In May 1985 an accident occurred to an Australian registered Bell 47 aircraft when one main rotor grip failed in flight and the blade separated from the aircraft. Investigation revealed /12/ that the blade grip had suffered a fatigue fracture through the wall of the internally threaded barrel section which accepts the retaining nut. The grip was manufactured from an aluminium alloy 2014 forging, the hardness being consistent with a T6 temper.

The failed grip is shown in Fig. 9.13. The macroscopic features of the fracture surface clearly indicate that fatigue had initiated at numerous sites around the circumference of the bore at the root of the thread run-out. Although fatigue cracking progressed outward around the entire circumference of the bore, cracking progressed more rapidly in two directions and formed two semi-elliptical fronts. One front extended outward, symmetrical about a horizontal axis, toward the pitch horn keyway at an angle of approximately 45^{o} to the wall of the bore. The other front extended outward, also at an angle of approximately 45^{o} in the quadrant bounded by the upper surface and the drag brace attachment lugs. The fracture surface is shown in Figs 9.14 and 9.15.

The crack which extended towards the pitch horn keyway was contaminated with a grey/black grease-like substance, which was identified as similar to the grease remaining in the stud holes. Progressive positions of the crack front were highlighted by the grease deposits, indicating that the grease infiltrated the crack as the crack front extended through the stud holes, prior to final failure. Yellow chromate-containing paint which was present in the pitch horn keyway also appeared to have penetrated into the crack before final failure. The presence of the paint on the fracture surface indicates that the crack front had intersected the root of the pitch horn keyway prior to reassembly at the last overhaul.

The threaded bore of the second grip from the accident aircraft was subjected to a rigorous inspection. A possible crack in the root of the first thread from the thread run-out was indicated by a fluorescent post-emusified dye penetrant inspection. However, eddy current inspection using a miniature probe located in a holder shaped to follow the internal thread indicated that two separate cracks were present in the first thread. Sections through these cracks are shown in Fig. 9.16. The two cracks were broken open and were found to be similar, in location, angle, direction of growth and surface characteristics, to the fatigue fracture in the broken grip. The maximum depth of the crack extending toward the pitch horn keyway was 6.3 mm and the maximum depth of the crack present in the quadrant bounded by the upper surface and the drag brace attachment lugs was 6.1 mm.

Since this was the first known occurrence of this type of cracking in the entire Bell 47 operating history (nearly 40 years), it was at first thought to be related to the severity of this aircraft's particular operational role (cattle mustering). However, subsequent inspection of a number of other grips, some of which had been retired from service as fatigue-life-expired, and many of which were still in service, showed that a large proportion contained fatigue cracks. Crack sizes ranged from microscopic, through to massive (ie almost at the point of failure), after times in service ranging from 1200 hours to the 5000 hours retirement life. These grips came from helicopters in all operational roles, showing that the problem was not confined to cattle mustering.

In order to contain the problem, the manufacturer reduced the retirement life from 5000 to 1200 hours. It is interesting to note that, from the known world-wide active Bell 47 fleet size, the known average annual utilisation, and the 5000 hour retirement life, the manufacturer estimated that the whole fleet of aircraft should have consumed approximately 1800 grips in the previous 5 years. The number actually delivered, from all sources, totalled 500.

During the course of the Australian investigation, Department of Aviation NDI specialists developed an effective and reliable eddy current inspection technique, which is detailed in the Appendix. This required the use of a special probe to fit the internal thread of the grip, as shown in Fig. 9.17. By implementing eddy current inspections at 1200 hours, and repeating at intervals of 600 hours, Australian operators are assured of crack-free grips for the full 5000 hour life. A number of other Airworthiness authorities have taken similar action.

9.3.8 Robinson R22 Fin Failure

In September 1986 a Robinson R22 helicopter crashed after the complete tail rotor assembly separated from the tailcone in flight. The cause of the failure is still under investigation. However, fatigue cracks have been found in the horizontal stabilizer channels which form the attachments for the lower vertical fin /13/. It is possible that the fin separated first and was struck by the tail rotor.

Since this was the second report of this type of defect (the first was received in 1985), this Department issued an urgent Airworthiness Directive to institute regular inspections of the channels. At the same time, the manufacturer and the FAA were notified. Typically, the fatigue cracks initiate at multiple origins on the outer surface of the aluminium alloy sheet material, near the edges of the anchor nuts, Fig. 9.18. No particular stress concentrations are apparent at the crack initiation sites. Microscopic examination of the fracture surfaces has shown that crack growth occurred under variable amplitude spectrum loading conditions.

The manufacturer has recently issued a service bulletin, which puts forward four possible causes for the cracking:

(a) idling at 60 to 65% RPM which places the stabilizer and fins in resonance with the tail rotor;

(b) tail rotor out-of-balance;

(c) tail rotor teeter hinge bearings worn and loose allowing tail rotor to go out-of-balance;

(d) insufficient clamping from bolts attaching vertical fins to horizontal stabilizer allowing fretting to occur in the joint.

The service bulletin requires a one-time inspection for cracks and a mandatory modification. It is expected that the FAA will issue an associated AD.

However, it is felt that the fatigue effects of normal aerodynamic loads cannot be ruled out without more detailed investigation. Further, there are some reservations as to whether a manufacturer's modification can be relied upon to give adequate protection against future fatigue cracking, especially on those aircraft which had accumulated significant, but undetectable, fatigue damage at the time of its installation. It is therefore intended that the 100 hour repeat inspections specified in the Australian AD will remain until the concerns outlined above are satisfied.

9.3.9 SA330J Puma Tail Rotor Blade Failure

An SA330J Puma helicopter was involved in a fatal accident following an in-flight failure of a tail rotor blade at 4150 hours. The blade failed because of a fatigue crack which initiated from a mechanically produced flaw, and subsequently propagated through the spar cap, as shown in Fig. 9.19(a), in less than 200 hours. Fig. 9.19(b) shows a scanning electron micrograph of the fracture surface, with distinct fatigue striation markings which are believed to correspond to the tail-rotor start-up cycles.

The blade failure provides an interesting insight into fatigue related airworthiness practices. Previously the blade was life-limited on the basis of the manufacturer's calculations at 6600 hours. Taking the current failure, and the many hours accumulated by other blades in service without failure, the maximum likelihood principle was used to establish a

mean blade life to failure of 20,000 hours. With an appropriate scatter factor, the safe life is around 6400 hours, in excellent agreement with the present retirement life of 6600 hours.

To provide adequate airworthiness control for the problem area, the blades in service are now being inspected every 50 hours, up to the compulsory retirement life for the complete blade. Inspections are being made for spar cracking using a low frequency eddy current (LFEC) technique. Use of this technique is in contrast to proposals from other aviation regulatory authorities which are prescribing a high frequency eddy current technique to detect early skin cracking. Particular care is being taken to ensure that the LFEC field equipment being used is fully responsive to the sought spar cracking.

9.4 FATIGUE DAMAGED STRUCTURE : DETECTION, ANALYSIS AND REPAIR

9.4.1 Fatigue Life Enhancement (J.Y. Mann - ARL)

Cold expansion of bolt holes was one of the techniques used to improve the fatigue lives of the wing main spars of the RAAF Mirage IIIO fighter aircraft. This particular application involved thick sections (up to 34 mm), and during the ARL investigations it became apparent that there was insufficient knowledge relating to the use of the process under these circumstances. Consequently, a programme of research was undertaken which included finite element and experimental investigations of the stress and strain fields around cold-expanded holes in thick sections of aluminium alloy complemented by fatigue testing, crack propagation studies and fracture analysis. The particular process studied was the split-sleeve cold expansion process marketed by Fatigue Technology Inc., Seattle, USA. Aluminium alloy A7-U4SG (equivalent to 2214) was used as the test material.

Resistance strain gauges and a microgridding/replicating technique /14/ (Section 9.4.6) have been successfully used to measure the surface strains around holes at the cold-expansion mandrel inlet and outlet faces, and also within the shear discontinuities (typically 2 to 3 mm long) caused by the split in the disposable sleeve. Figure 9.20 indicates the extent of the deformation at the hole associated with the split in the sleeve, and Fig. 9.21 the progressive change in strain at the inlet face of a 15 mm thick specimen during mandrel insertion. Between the shear discontinuities the hoop and radial strains (on both faces) are almost zero, while on the side of the hole opposite the shear discontinuities the magnitudes of the hoop and radial strains are considerably greater on the inlet, compared with the outlet, face /15/. This is shown in Fig. 9.22 for 23 mm thick specimens.

Measurements of the z-direction out-of-plane displacements at the mandrel inlet and outlet faces have indicated, for 15 mm thick specimens, that these are considerably less at the inlet face than the outlet face, Fig. 9.23. In a multiple-stack hole cold-expansion situation the z-direction displacements depend on the materials in contact. For example, in the central aluminium component these displacements become progressively less for single thickness aluminium alloy, three layer aluminium-alloy stack and steel/aluminium-alloy/steel stacks /16/. Furthermore the z-direction displacements are significantly less for 8 mm thick specimens than for those of 15, 23 and 30 mm.

Fatigue tests (under a flight-by-flight sequence used for the Mirage investigation /17/) have been carried out on open hole specimens of 8, 15, 23 and 30 mm in thickness with a hole of about 8.6 mm diameter; and on low-load-transfer bolted joints in which the holes were cold-expanded either in a single thickness of material or concurrently as part of an aluminium-alloy/aluminium-alloy/aluminium-alloy stack or a steel/aluminium-alloy/steel stack. In these joints the aluminium alloy in the centre was 15 mm thick.

The increase in fatigue life as a result of cold expansion is significantly less for 8 mm thick specimens compared with those of the other thicknesses - 4:1 against 6:1 relative to non-cold-expanded holes. There is also a progressive change in the development of fatigue cracking with an increase in specimen thickness - from an almost "through" crack in the 8 mm case to a bulbous shape at the mantrel inlet face of the specimens of thickness 15, 23 and 30 mm (Fig. 9.24). There is clear evidence that, in the latter group, cracking propagates more rapidly at the mandrel inlet face of the specimen than at the outlet face in the latter stages of crack growth. Fatigue tests on 23 mm thick specimens indicated that split-sleeve orientation, post cold-expansion reaming and the removal of the z-direction out-of-plane displacement had no significant effects upon the fatigue lives of cold-expanded hole specimens /15/. Compared with non cold-expanded holes the life ratio was between 6 and 7.5 times greater. It also appeared that, when the sleeve was

oriented on the transverse axis of the hole, the fatigue cracking initiated later along the residual ridge than on the side opposite the split. This is very surprising in view of the severe deformation adjacent to the ridge along the hole.

Cold expansion of open-hole specimens provided significant increases in life (by factors of about six) irrespective of whether it was done in a single thickness of aluminium or as part of a multi-layer stack-up /16/. Much smaller increases in life (a factor of about two) were found for the bolted-joint specimens, and the differences (for the two types of specimen) were attributed to the detrimental effects of fretting in the latter.

Fatigue crack growth studies on specimens, the holes of which were cold expanded after the development of fatigue cracks, have confirmed that rapid crack growth occurs in the first 10% of the life followed by a much reduced (but constant) rate until about 75% of the total life, after which it accelerates until failure. Little difference in total lives to failure was found between specimens with holes cold-expanded before fatigue testing and those cold-expanded after the development of small fatigue crack.

There is also some preliminary evidence that, for similar failing loads, the fatigue cracked areas of specimens with cold-expanded holes are considerably greater than those with non-cold-expanded holes. These findings are of some importance in damage and durability analysis and are to be investigated in more detail.

9.4.2 Stress Analysis of Cold Expanded Holes (G.S. Jost, R.P. Carey - ARL, G.P. Steven - UOS)

The application of finite element analysis to cold-expanded holes, reported in the previous Review, has been continued and expanded. At ARL a hole in a large circular aluminium alloy plate having a bilinear stress-strain relationship has been cold expanded first to that point (1.63%) which, upon relaxation, leaves the material at the hole on the incipience of reverse yield /18/. The hole has then been expanded further, and relaxed, to 2%, 3%, 4% and 5% of diameter under both plane stress and plane strain conditions. Examples of graphical output are shown in Figs 9.25 where attention is drawn to the out-of-plane stress distribution for the plane strain case and the out-of-plane strain for the plane stress case. The work is being repeated, in the first instance, for the three-dimensional case where the thickness is equal to the hole diameter. Although the outcomes might be expected to fall between the two-dimensional extremes, significant deviations may occur /1/.

In a parallel investigation at the University of Sydney which included substantial software development, finite-element analysis is being used to determine stress and strain fields in a rectangular plate containing a cold-expanded hole. In this case the Ramberg-Osgood stress-strain characteristic closely represents that of an aluminium alloy. Expansions of up to 5% have been simulated as above using small displacement theory /19/. In addition, for the 5% case, the analysis has been repeated using large displacement theory: the resulting differences in predicted stress fields are not insignificant, Fig. 9.26, /20/. Immediate next stages in this study will include the influence of remote loading and pin (fastener) loading in conjunction with neat-fit and interference-fit fasteners in the cold-expanded hole.

9.4.3 Use of Adhesive Inserts to Extend the Fatigue Life of Cracked Fastener Holes (M. Heller, R. Jones - ARL, J.F. Williams - UOM)

In aircraft wings the aerodynamic loads are transferred from the wing skin to the spars by means of bolted and rivetted joints. These joints are one of the main causes of cracking and often determine the fatigue life of the structure.

Although recent studies have shown that the use of solid bonded inserts can significantly increase fatigue life, this has been done on uncracked holes and the numerical analyses, /21/, have concentrated on holes containing cracks unrepresentative of realistic damage.

Accordingly, this project is investigating the on-site repairability of holes containing existing, real cracks by bonding into the hole a (stiffer) steel sleeve using epoxy resin and avoiding the (current) necessity of having to return the structure to a major depot for reworking. The use of a sleeve, of course, minimises the opening and closing of the crack under repetitive fatigue loading and also allows the rivet or bolt to be inserted or removed as desired.

The project is being carried out in two parts:

First, a series of experiments have been performed on pre-cracked specimens in both the repaired and unrepaired conditions at constant amplitude loading to determine their respective fatigue lives. The reason for doing this was to establish that the method will work for holes containing existing cracks and to establish the maximum crack size that can be successfully repaired by this method.

Secondly, a detailed stress analysis of the repair procedure is being undertaken to identify the key parameters with the aim of optimizing the method. As expected, the stress analysis, using finite element techniques, has indicated that adhesive bonding significantly reduces both the local stress concentration at the hole and the stress intensity at the crack tips thus retarding the growth rate of potential fatigue cracks.

9.4.4 A Study of Three-Dimensional Crack Growth in Metals (J.F. Williams - UOM, R. Jones - ARL)

LEFM has primarily been concerned with crack growth and subsequent failure in two-dimensional (plane strain/plane stress) situations. However, most failures are three-dimensional in nature. Several methods are now available for evaluating the variation of S and K_I around the crack front. These methods are being investigated and compared to experimental and numerical values for a typical surface flaw.

Methods for calculating the energy release rate, G, in three-dimensions, now appear to require a critical overview. It seems that the value of the local G may depend on the way in which it is evaluated, namely, should G be calculated over a finite but small area or, as is currently done, at a point?

9.4.5 Experimental Stress Measurement (J.G. Sparrow - ARL)

Work has continued on the measurement of stress using the SPATE 8000 thermoelastic stress analyser /22/. The instrument has been used for the stress mapping of specimens during cycling in electro-hydraulic fatigue testing machines, of aircraft components under test in the laboratory /23, 24/ and of high stress regions of aircraft under field conditions.

The instrument was designed to detect the small temperature changes occurring during cyclic loading of a specimen. The thermoelastic constant relates these temperature changes to the changes in the sum of the principal stresses. Recent work has shown that the thermoelastic constant is dependent upon the mean stress about which the cyclic stress is imposed /25, 26/. A theoretical explanation of the mean stress effect has been developed /27/. This dependence suggests a potential application of the thermoelastic effect in the measurement of residual stresses.

The use of ultrasonic shear wave birefringence as a means of measuring residual stresses is also being investigated /28-30/. Recent work has concentrated on improving the data transfer rate to the main frame computer and development of analytic programs. Other methods of stress measurement being studied include moire fringe techniques (shadow and in-plane) /31,32/ and holographic interferometry /33-36/. These optical methods are complementary to the use of direct measurements of the displacement of fine grids, a technique developed for the study of the plastic strains in the vicinity of crack tips and cold-expanded bolt holes (see Section 9.4.6).

9.4.6 Microgridding Technique and Applications (P.W. Beaver - ARL)

The fatigue and fracture properties of most engineering metals and components are determined by the localised plastic deformation that occurs in the vicinity of defects, such as crack tips and/or geometric discontinuities, such as holes. In this research a method of accurately determining the local plastic strain distribution in the vicinity of crack tips and holes has been developed /14,37,38/. The method involves the application of a very fine square microgrid pattern (typically 25 μm line spacing) to the area of interest. The local plastic strain distributions, produced by either static or cyclic loading, are determined from replicas of the deformed grid pattern taken whilst the specimen is under load. The grid point displacements are measured from the replicas using an optical microscope and an image analysing system, and are converted to strains using a computer which outputs the data in a variety of graphical or numerical forms.

This microgridding and replicating technique has been used in several areas of research into the fatigue and fracture behaviour of aluminium alloys used in the aircraft industry. The first application was to determine the elastic-plastic fracture mechanics parameter, J /39/. This parameter is a measure of the intensity of the plastic stress and strain field at the crack tip. Initial static crack extension occurs when J exceeds a critical value J_{IC}. The J_{IC} value for a medium strength aluminium alloy, 2024-T351, was determined using a theoretical model for representing crack tip plastic stress and strain fields, and the strain values determined from replicas. (Fig 9.27 shows examples of replicas just before and just after initial static extension.) This J_{IC} value was compared with the values obtained from two numerical methods and the ASTM standard test method. Agreement between these values was good, Table 9.2. The 95% confidence intervals for the various methods overlap indicating that the differences between the J_{IC} values are due to material variability and experimental scatter.

An important part of the ASTM standard J_{IC} test method is the measurement of the amount of crack extension as a function of load. The usual method of marking crack fronts in aluminium alloys for subsequent measurement is to fatigue cycle after the initial static crack extension. A new method of marking crack fronts, based on liquid metal embrittlement of grain boundaries in aluminium by gallium, was developed during this research programme /40/. This method was more effective than the usual fatigue cyclic method for the aluminium alloys examined in this work.

The effects of parameters in the fatigue loading cycle, such as mean load and amplitude, on crack tip strain distribution, and hence fatigue crack growth rates were also determined /41/. Figure 9.28 shows examples of crack tip strain profiles. The numerical data showed that for aluminium alloy, 7475-T7351, the fatigue crack growth rate in the stage II region is related to the effective crack tip plastic strain range by the following equation:

$$da/dN = C\ (\Delta\varepsilon^{p}_{effective})^{n}$$

where C = 228 μm/cycle and n = 2.16. This relationship is independent of the R-value. The dependence of the da/dN vs K relationship on the R value suggests that a linear relationship between ΔK and $\Delta\varepsilon^{p}_{effective}$ does not exist. Work is in progress to use the crack tip strain data to model fatigue crack growth in metals and components. Effects such as delayed retardation in growth rates as a result of overloading will be included in the model.

9.4.7 Multiaxial Fatigue (P.W. Beaver - ARL)

Literature surveys on the influence of multiaxial stressing on the fatigue and fracture behaviour of both metals and fibre-reinforced composites have been completed /42-44/. These surveys indicate significant biaxial load effects on the fatigue and fracture behaviour of both types of materials.

9.4.8 Fractography of Fatigue Cracks in F-111 Wing Pivot Fittings (A.F. Cox - ARL)

Continuing concern about the presence of fatigue cracks in critical components in F-111 aircraft of the RAAF has led to a need for information to be acquired about crack growth rates and characteristics. The components of interest are large forged, welded and heat-treated wing pivot fittings which attach the wings to the carry-through box in the fuselage centre-section, Fig 9.29. These fittings are manufactured from a high-strength steel which by virtue of its low fracture toughness can tolerate cracks only a few millimetres in depth. Figure 9.30(a) shows a crack which led to catastrophic failure under test loading. Inspection programs have been introduced which will detect the presence of cracks with surface lengths of only a fraction of a millimetre, although the size and complexity of this component makes development and implementation of NDI programs particularly difficult.

It is essential to determine the growth rates of cracks which have been detected if appropriate inspection intervals are to be established. This information has been acquired by the use of quantitative fractography - by correlating the fracture surface fatigue markings with the known load history of the individual aircraft, the crack size and shape may be established at a number of points and times corresponding to known events in the flight load history. Typical results obtained by matching fatigue progression markings with flight numbers is shown in Fig. 9.30(b) The information obtained by the use of advanced quantitative fractographic methods has played an essential role in the assessment of these defects, and is currently being used in the formulation of appropriate inspection programs.

9.4.9 A Test of Some Fatigue Crack Growth Prediction Models (J.M. Finney - ARL)

Four load-sequence-effect models, Wheeler, Willenborg, Modified Willenborg and Crack Closure, were examined for their effectiveness in predicting fatigue crack growth. Predictions from the models were compared against experimental crack growth data obtained from tests on centre-cracked specimens of 2214-T651 aluminium alloy /45/. Four sequences, each at two stress scaling levels, were applied to the specimens. The basic load sequence was a flight-by-flight fighter sequence and, after range-pair counting, three other sequences were generated each giving the same range-pair table. One reconstituted sequence was fully random, a second aimed to accelerate crack growth, while the third aimed to retard crack growth.

Over the four sequences and two stress scale levels the order of increasing predicted crack growth life is practically the same, namely Unretarded, Wheeler, Modified Willenborg, Willenborg, Crack Closure, as illustrated in Fig. 9.31.

The Wheeler model is preferred overall because :

(a) it gives the best predictions of crack growth for the more random (random and flight-by-flight) sequences, and is therefore the most suitable for many practical applications.
(b) its predictions are not more than a factor of 1.7 from any of the experimental data.
(c) it tends to err conservatively.

None of the models correctly predicts the trends in experimental crack growth obtained over the four sequences.

Table 9.3 shows that the predicted crack growth lives for the two less-structured sequences, random and flight-by-flight, are practically the same for any given model - the maximum difference is only 5% - and this correlates well with the ratio obtained experimentally. In broader terms the same can be said of the two more-ordered sequences, acceleration and retardation. However, experimentally, the acceleration sequence gave the longest crack growth life and the random sequence gave the shortest, yet all of the models predict the reverse trend.

9.4.10 Load Cycle Reconstruction (J.M. Finney - ARL)

An experimental programme /46/ has investigated the range of crack growth lives that may be obtained by various reconstitutions of a range-pair counted flight-by-flight fighter sequence. Previous work had shown that, for bolted specimens, there was no difference in total life for sequences reconstituted to either accelerate or retard crack growth.

Centre-cracked specimens of 2014-T651 aluminium alloy were tested under the original flight-by-flight sequence, a fully random reconstituted sequence, a sequence to accelerate crack growth (sequence A2) and a sequence to retard crack growth (sequence R2). Three specimens were tested under each sequence at each of two stress levels (11.0 and 17.0 MPa/g), and the results are shown in Figs. 9.32(a) and (b).

The conclusions that may be drawn from these results are as follows :

1. At long lives (about 40 programmes or 20,000 flights at 11.0 MPa/g) there is no significant difference in crack growth for the acceleration and retardation sequences. At shorter lives (about 10 programmes or 5000 flights at 17.0 MPa/g) the retardation sequence gives significantly faster crack growth than the acceleration sequence, but the difference is relatively small, only 15%.
2. Crack growth lives under the flight-by-flight and random sequences are practically identical.
3. Crack growth under the more-structured sequences (A2, R2) is significantly slower than under the less-structured more-fluctuating sequences (random and flight-by-flight).
4. The maximum spread in average crack growth lives is between those from the acceleration and random sequences at both stress levels and is an average of 1.59 : 1 at 11.0 MPa/g and 1.51 : 17.0 MPa/g.

The dominant factor producing the small variations in crack growth life was the frequency of load level changes, and the sequences designed for crack growth extremes were deficient in this respect. Preliminary fractographic analyses indicate that local retardations and accelerations in crack growth did occur under sequences R2 and A2 but they tended to average out over the lengthy sequences used. Although the variations in crack growth life were rather small

compared with other uncertainties in crack growth assessment, to be conservative, random or flight-by-flight reconstitutions of aircraft load spectra are recommended for testing purposes.

9.4.11 Fatigue in Structures Containing Several Cracks (D.G. Ford - ARL)

A computer program is being developed at ARL to predict the fatigue life distribution of a structure with several interacting critical regions.

For each of these regions the fatigue process is divided into pre- and post-cracking stages, and existing cracks affect fatigue in other regions through stress redistribution. The life distribution follows from a reliability analysis of the range of possible crack-growth histories of the structure.

This is the model described by Ford /47/ in 1984. Its implementation has exposed several numerical problems but also allowed significant generalisations which would be intractible in an analytical treatment. The generality of the program, which reflects the variety in the fatigue process, means that more information must be fed in to obtain results. In present practice much of the same information is supplied at different stages of an analysis but important effects can be missed thereby. Additional input specific to the program describes stress models used, the interaction between cracks and strength or fracture in the presence of several cracks.

It was found that the contributory models in the program could be related to loads, S-N data and crack growth. Information under these headings is supplied for each crack and the use made of it depends on the (compatible) choice of user-supplied or internal models. The general philosophy of internal modelling is to fit a robust model to the supplied data and then fit bicubic splines to residual effects.

For this purpose optional internal models are included for low cycle fatigue and crack growth. It was also found necessary to devote considerable attention to range pair data in order to adequately smooth load sampling. The program has special provisions for repeated use of the same or similar data at several crack sites.

Interaction between cracks implies that the development of failures can only be followed dynamically. In the current version of the program short-term local randomness of cracks is neglected and the mathematical problem reduces to a first order continuity equation for crack length probability. This is not determined explicitly, but the characteristics are followed using standard Adams-Bashforth integration over equal time intervals. To reduce fatigue-type computation special starting procedures were developed, avoiding partial steps but starting with second derivatives in a one-step predictor-corrector routine. (Each "crack" has at least two "starts", for failure probability and actual crack initiation. Inspections can increase this number.)

The generalisations with computational solutions are the inclusion of inspections and the confluence of cracks to form fewer, more dominant failures. Obviously the geometric and stress-dependent details for these must be user-supplied. Other required subroutines describe the stress fields with crack interaction, the corresponding strength, repair schemes and inspections. In principle, direct stress analysis and fracture mechanics could be included but it is felt that summarised information would be more practical and efficient.

9.4.12 Range-Mean-Pair Exceedances in Stationary, Normal Fatigue Sequences (D.G. Ford - ARL)

In fatigue, range-mean-pair (or rainflow) counts correspond to closed hysteresis loops so that their distributions affect initial lives in low cycle fatigue. They are also useful empirically in general life and crack rate prediction.

Many fatigue problems arise from random loading of linear structures for which the stress response is often stationary and Gaussian. Examples are oil rig platforms, vehicle suspensions and turbulence loading of aircraft. This implies that the relation between range-pair counts and the power spectrum or autocorrelation of a stationary Gaussian process is a central problem in fatigue prediction which has been addressed at ARL.

The method used is an extension of the finite dimensional procedure for level crossings as described by Cramer and Leadbetter /48/. In this the continuous process is treated as the limit of a discrete process. Rainflow exceedances,

which are more easily analysed than count densities, are characterised by directed crossings of the two defining levels. However time or frequency information also requires a third crossing to define a recurrent event.

The general procedure is therefore to predict the frequency of triple crossings equivalent to the range-pair exceedance. The length of each such event consists of two first passages from one defining level to the other. With suitably conditioned probabilities these are again established from recurrent event theory. A Pascal program is being developed for estimating exceedances for range-pair tables.

The work done so far is described in /49/ and an overview of the project has been presented at /50/.

9.4.13 Crack Patching - Technology Base Studies (A.A. Baker - ARL)

Developments have continued in crack patching technology for fatigue or stress corrosion cracked metallic components. As first described in the Australian ICAF review in 1977, crack patching technology is generally based on boron-epoxy patches and structural film adhesives. Aspects described here (given in more detail in /51/) include (i) a preliminary design approach and (ii) fatigue crack propagation studies. Other topics covered in /51/ include: (a) evaluation of minimum conditions for bonding of repair patches; (b) discussion on potential residual stress problems, arising from mismatch in expansion coefficient between the metal and patch and (c) estimation of stress intensity in patched panels.

9.4.13.1 A Preliminary Design Approach

The main aim of the design approach is to provide a feasibility assessment of repairability of a cracked component and, if repair is feasible, to provide estimates of :

(a) minimum required patch thickness
(b) minimum required bond overlap length
(c) expected durability of the repair scheme
(d) conservative value for the reduction in stress intensity.

The approach taken to estimate minimum patch thickness, illustrated in Fig.9.33 in flow chart form, is based on comparison of (i) the computed overlap length L_R for the patch with the allowable length L^*, (ii) the computed peak strain in the patch e_R with the allowable strain e_R^* and, (iii) the computed shear strain range $\Delta\gamma_A$ in the adhesive with the allowable $\Delta\gamma_A^*$.

The composite patch is increased in thickness one ply (about 0.13 mm) each cycle and the values of e_R and $\Delta\gamma_A^*$ are taken from tests on representative lap joints /51/. In this design approach no attempt is made to design to a specified stress intensity. However, the resultant stress intensity following patching, ΔK_∞, is estimated and compared with the initial value ΔK_a. The analysis accounts for residual stress σ_T resulting from expansion mismatch between the patch and cracked component and curing temperature range ΔT. The results of an example analysis are provided in Fig.9.33.

9.4.13.2 Fatigue Crack Propagation Studies in Patched Specimen

General considerations

Effective patching is expected to have two major beneficial effects in reducing crack growth. It should (i) retard the reinitiation of the crack, and (ii) reduce the rate of crack growth once growth resumes. Both effects result from the reduction in stress intensity range from ΔK_a for the unpatched specimen, to ΔK_R, the effective value following patching - ideally equal to or less than ΔK_∞, the maximum predicted value.

Essentially, retardation is associated with the formation of a plastic zone at the crack tip during loading. The plastic zone acts as an oversize inclusion, resulting in a compressive residual-stress from the surrounding elastic material when the external loads are removed. When a patch is applied the peak stress intensity is reduced from K_a to K_R. However, the opening of the crack tip will be very much less than would normally occur at K_R due to the compressive residual stress field. The onset of further plasticity at the crack tip will similarly be greatly reduced. Since, during cyclic loading, the damage per cycle is dependent on the size of the plastic zone formed during each cycle, the result of patching is a marked reduction in the size of the plastic zone associated with each cycle and hence a corresponding

reduction in crack growth rate, until the crack grows out of the region of the original (pre-patching) plastic zone. Even under service (variable) loading, some retardation effects would be expected, depending on the stress level imposed on the component immediately prior to patching.

Following patching, and after retardation effects on growth are exhausted, the reduction in the rate of crack growth reflects the reduction in stress intensity range. Further, since (as previously discussed in /52/) patching theory predicts that the stress intensity K_∞ following patching should be independent of crack size, the rate of growth da/dN is expected to be constant in accordance with the empirical relationship $da/dN \propto (\Delta K)^n$ where n is an exponent generally of the order of 3 to 4.

Finally, two potentially important complicating factors must also be considered. The first is the presence following patching of the thermally induced residual stress and the second is the influence of heat-treatment following patching on the behaviour of the cracked component.

Crack propagation studies

Edge-notched specimens, as depicted in Fig.9.34 (inset), were subjected to cyclic loading at constant load amplitude. In this work two similar specimens are simultaneously tested while joined together to form a honeycomb panel, with the patched sides facing outwards. The aim of this configuration is first to minimise curvature, caused by the residual stress following patching: patches are usually bonded at the same time as the panels are bonded to the honeycomb core. The second aim of the configuration is to minimise bending of the panels which would otherwise occur during testing; the moments which cause bending arise from the displacement of the neutral axis of the metal panel by the patch. The support provided by the honeycomb panel configuration is considered to be a reasonable simulation of the support that would be provided in typical military aircraft structure.

Crack growth in the patched panels was monitored through the patch using an eddy current procedure and, following testing, the panels were subjected to X-ray radiography (using an X-ray absorbent fluid, tetrabromoethane) to detect disbonding or delamination of the patch. In most panels no evidence of significant disbonding or delamination was found - this finding was later confirmed by metallographic observations on prepared sections.

Some of the findings and conclusions from these crack propagation studies are as follows:

(i) Patching efficiency is very high, as shown in Fig.9.34 which compares crack growth data for typical patched and unpatched specimens tested under the same nominal loading conditions.

(ii) Significant retardation in crack growth is experienced with the longer (25 mm) starting crack, but none with the shorter (5 mm) starting crack. This difference in behaviour between the two crack sizes can be explained as follows: the degree of retardation of crack-growth following patching depends on the reduction in stress intensity range from ΔK_a to ΔK_R. Since the minimum stress intensity range ΔK_R is expected to be independent of crack size, the reduction in stress intensity range for the large crack and hence the degree of retardation is much greater than that for the small crack.

(iii) Crack growth da/dN under the patch follows a parabolic relationship in some cases - see for example the short crack in Fig.9.34 This implies that ΔK_R for the patched specimen is not totally independent of crack length a.

(iv) The degree of retardation is significantly reduced when relatively high temperature treatments are used. This behaviour is evident in Fig.9.35 It appears likely that the heat-treatment relaxes the level of elastic constraint acting on the crack, probably by a process of creep recovery in the plastic zone.

(v) Use of an adhesive (FM300 - by Cyanamid) curing at the highest temperature (175°C) leads to a moderately increased rate of crack growth. This is probably due to the higher level of residual stress when the patch is applied at 175°C. Further reference to Fig.9.35 shows that, when the patch is applied at 120°C followed by heat-treatment at 175°C, no increase in growth rate is evident - even though the degree of retardation is similar. The theoretical value of residual stress following patching with adhesive AF126 is about 67 MPa whereas with adhesive FM300 it is about 102 MPa.

9.4.14 Boron/Epoxy Doublers for F-111 Wing Pivot Fitting (B.C. Hoskin, A.A. Baker, R. Jones - ARL)

At the request of the RAAF, ARL is undertaking the development of boron/epoxy doublers to improve the fatigue performance of the F-111 wing pivot fitting upper plate region; this part is made of D6ac ultra-high strength steel. Whilst ARL has considerable experience in the use of bonded composited repairs for metal aircraft structures, the present development is more advanced than any undertaken in the past, primarily because these doublers are much thicker than any used previously.

Extensive finite element design studies have been undertaken and a detailed evaluation of the materials engineering aspects has been made. Procedures for applying the doublers to the wing in situ have been developed and particular attention has been given to thermal mismatch problems. The RAAF provided a salvaged wing from a crashed F-111C and this has been repaired by HDHV to a state suitable for structural tests. Using a rig, Fig.9.36, built by HDHV, where loads can be applied to the test wing as in the standard F-111 cold proof load test, strain surveys of the wing pivot fitting have been made before and after application of the doublers. It has been confirmed that substantial reductions in the strains in the fatigue critical regions are achieved with the doublers. This development is still in progress.

9.4.15 Combined Fatigue/Environmental Box Beam Test (K. Watters - ARL)

A 2.5 m long box-beam specimen is currently being fatigue tested. The box-beam comprises a 56 ply XAS/914 graphite/epoxy skin (28 plies at 0^{o}, 28 plies at $\pm 45^{o}$) attached by titanium fasteners to an aluminium alloy and steel substructure. The cross-section is shown in Fig.9.37. The main aim of the test is to examine the growth of barely visible impact damage in the composite skin, including the effects of moisture absorption and temperature excursions. A FALSTAFF loading sequence, with low loads truncated, is being used for the fatigue test. The loading configuration is three-point bending causing compression in the composite skin.

Prior to fatigue testing, the mid-span region of the composite skin was extensively strain gauged and a static strain survey was performed. The composite skin was then deliberately damaged at a total of seven locations in the mid-span region by impacting it with a free-falling mass. Impact energies ranged from 12J to 35J and impact locations were over spars, adjacent to spars, and midway between spars. In all cases the damage fell into the barely visible category with only small indentations being visible on the outer surface. The extent of sub-surface damage measured by C-scan is shown in Fig.9.38.

After being damaged, the box-beam was subjected to one lifetime of fatigue loading (30 blocks of the FALSTAFF sequence or 6000 hours) under laboratory ambient conditions. No damage growth was detected. The box-beam is currently being conditioned in a hot wet environment to achieve 1% moisture content in the composite skin.

Following moisture conditioning fatigue loading will be resumed. This second phase of fatigue loading will be performed under a controlled temperature spectrum which includes cold, room and high temperature segments and a significant number of freeze-thaw cycles. Under high load level and high temperature, load dwells will be included to simulate real-time loading rates. The segment of the FALSTAFF sequence to be used for high temperature testing will be chosen to maximise the correlation between high loads and high temperature.

9.4.16 Failure Characteristics of Laminates Containing Pin-Loaded Edge Holes (J.F. Williams, T.E. Tay - UOM)

It is well known that in fibre composite materials the location of maximum stresses, and the failure mechanisms associated with these stresses, occur in quite different regions and by different modes than is predicted by conventional theories for isotropic, homogeneous materials.

Using finite element analysis methods, an investigation is currently underway to examine the stress fields and failure mechanisms in the vicinity of a hole near the edge of a semi-infinite graphite/epoxy plate loaded in tension, perpendicular to the edge of the plate.

To date the analysis has revealed that two regions are possible sites of initial failure:

(i) the first type of failure mode appears to be a type of bearing failure at the midpoint of the loaded edge of the hole. In this case, "bearing" failure is not to be associated with the normal compressive overload situation in isotropic materials. With fibre composites, the problem is more associated with excessive shear stresses arising at the contact (or bearing) surface, causing breakdown of the matrix in plies aligned at 45^{o} to the line of load application.

(ii) the second type of failure appears to be shear failure in the matrix occurring at points symmetrically located on either side of the hole at approximately 60^{o} away from the line of load application and at the edge of the hole.

The Tsai-Hill and the Tsai-Hoffman failure criteria are being applied to the problem and will be compared to results from a variety of experimental tests.

One aim of this investigation is to examine the effect of edge proximity on the stress distribution surrounding the hole. In addition, Nuismer's point stress criterion will be evaluated.

9.4.17 Defect Repair in Fibre Composite Materials (R. Jones, J. Paul - ARL, J.F. Williams - UOM)

Repair to damage in composites must include a consideration of the materials needed to perform the task. The objective of a repair action is to restore the physical and mechanical properties of the component and allow it to function in its operational environment.

It is desirable to use materials similar to those used in the original structure. For example, repairs on graphite/epoxy composites typically utilize epoxy resins to fill delaminations and graphite/epoxy patch materials to repair large damage.

The project is considering two generic approaches to the problem of composite repair, namely bolted and bonded repair procedures. An advanced super-element is being developed to enable computational studies to be undertaken on the design of bolted/bonded repairs. The prime purpose of the computational work is to establish the mechanisms by which the repair restores strength to the damaged structure.

Further studies will also be undertaken in order to establish the reject/repair criteria for composite-to-metal joints.

9.4.18 Criteria for the Prediction of Compression Failure of Graphite/Epoxy Plates J.F. Williams - UOM, D.C. Stouffer - Univ of Cincinnati)

The need for a method of predicting the residual strength of composite materials comes as the result of rapid development in the aircraft industry which has created significant interest in this high strength-low weight material. One area of particular interest is the residual compressive strength of laminates containing either impact damage or interply delamination, /53, 54/.

The intention of the project is to assess the suitability of large deformation buckling theory, the finite element method and the techniques of fracture mechanics to determine the conditions under which a delaminated or damaged region may progress to structural failure.

In doing so, three project phases are in progress, viz:

(i) the determination of whether the propagation of a delamination can be treated as: (a) a small deformation crack-type mechanism with associated stress singularities at the crack tip or (b) as a non-linear, ie. large deformation problem involving debonding due to the resultant peel and inter-laminar shear stresses. Several experiments have already been performed on epoxy bonded aluminium laminates; the results seem to give evidence of both modes being present.

(ii) using the finite element program ABAQUS to evaluate the strain energy release rate G as a function of crack (delamination) length and to evaluate the stress distributions along the debond line. This has yielded some extremely interesting and controversial results, /55/.

(iii) once the appropriate failure mechanism has been established and analysis routines refined, tests and further analytical work on built-up, multi-ply specimens of T300 graphite/epoxy will be undertaken to enable rational design procedures to be evolved.

The significance of this research lies in the importance of being able to assess the degree of structural damage occurring in aircraft due to either accidental or military causes and in doing so help evolve appropriate safety inspection strategies. It will also contribute to the development of a properly based overall design rationale for these new structural materials.

9.4.19 Characterization of Failure Modes in Graphite/Epoxy Composites (R. Jones - ARL, J.F. Williams - UOM)

In order to apply LEFM to composite materials, there is a need to know the stress intensity levels within the matrix of the laminate. This is because crack propagation from existing flaws or damage will generally initially grow in the epoxy resin used to bind the fibre together. The problem is that, except for Sih's strain energy density theory, no satisfactory solution has been developed to allow a proper understanding of three-dimensional crack growth to be gained.

As a first approach, an investigation is being carried out to examine ways of verifying Sih's theory. This will be done by carefully designing a number of appropriate techniques to experimentally evaluate K_I, K_{II} and K_{III} at specific locations in a loaded composite plate. These results, together with a detailed finite element analysis of the problem will then be compared with the predictions of Sih's theory.

If this can be done successfully, it means that the use of Sih's theory together with valid measures of matrix fracture toughness in various geometrical configurations will provide a very much needed design rationale for those involved in the manufacture of fibre composite structures.

9.4.20 NDI Research (I.G. Scott - ARL)

Progress in non-destructive inspection (NDI) research has continued largely along the lines described previously but with the impending completion of some projects, new areas of work are being developed.

Analysis of results from acoustic emission (AE) monitoring of a full-scale fatigue test on a Mirage III aircraft has virtually concluded. It has been demonstrated that by adopting a semi-adaptive approach /56/ involving calibration using pencil lead fracture, by using broad band sensors and by collecting and analysing waveform data, it is feasible to collect and identify AE signals from growing fatigue cracks in the extremely hostile environment of the subject fatigue test. The results were confirmed from post-test fractography.

Basic studies of the eddy current technique have been continued and satisfactory progress has been made with study of the forward case (ie predicting coil response) in 2D and 3D. Analysis of wave propagation in plates has continued using in some cases computer codes made available from another Defence laboratory.

Australian research in NDT was recently reviewed in a paper provided to a conference on NDE of Advanced Materials and Composites /57/.

9.4.21 Developments in Practical NDI (G. Clark - ARL)

The application of non-destructive inspection methods to composite materials and components is an area of major interest, particularly with the acquisition by the RAAF of the F/A-18 aircraft. The potential long-term effects of impact damage occurring during service are not yet fully understood, and in order to assess the significance of such damage it is first necessary to develop NDI methods which can locate the damaged area and reveal its nature and extent. At ARL an ultrasonic technique, depth C-scanning, has been developed /58/ for use with a large immersion

ultrasonic system; this technique uses time-of-flight ultrasonic data, combined with a more conventional C-scanning approach, to determine both the extent and depth location of each delamination in the damaged region. A sophisticated data analysis and display system permits real-time display of defect maps which are colour-coded to assist with interpretation (Fig. 9.39); resolution is sufficient to allow layer-by-layer display of the damage envelope. This work is continuing, and is expected to assist considerably with more fundamental studies of damage and damage growth in composite materials, as well as with conventional NDI of metallic materials.

A portable version of the depth C-scanning system is being developed and this will permit the acquisition of ultrasonic signal data from impact-damaged coupons under test, or from damaged aircraft components in the field. These data can then be transferred to the larger system for more sophisticated processing, analysis and display.

Work is currently under way to investigate the feasibility of in situ NDI of critical components. Various approaches are under consideration, including eddy current, magnetic field leakage, and methods based on optical fibre fracture. The objective is to develop a sensor system which can be permanently mounted in known critical regions of an airframe and, by means of either real-time monitoring or signal storage, to detect the development of cracking. Areas in which critical defect sizes are small are of particular interest, and any useful approach must feature high levels of both sensitivity and stability.

9.4.22 Fatigue of Impact-damaged Carbon Fibre Composites

As part of a program to investigate the durability and damage tolerance of carbon-fibre reinforced components, tests have been conducted to determine the fatigue behaviour of impact-damaged carbon-fibre composite coupons representative of a fighter aircraft wing skin /59/. Coupons of XAS-914 were 300 mm x 100 mm, and 56 plies thick, with a gauge area of approximately 120 mm x 100 mm; the fibre layup was $[\pm 45/0_2]_{7s}$. Impact damage (12J) representative of that caused by a dropped tool was introduced using an indentor with a 12.7 mm diameter hemispherical tip. Testing was conducted using a compression-dominated FALSTAFF loading sequence, with a peak strain of -3750 $\mu\varepsilon$, representing a severe but not unrealistic flight loading condition. To prevent gross specimen buckling, appropriate restraints were used, and a shadow moire system was used to monitor growth of the damage during the fatigue test.

1984/85 Programme (G. Clark - ARL)

The initial program evaluated the influence of the low loads in the sequence on fatigue life; lives under the full FALSTAFF sequence were compared with those obtained using a modified sequence /60/ in which load transitions occurring entirely within FALSTAFF load levels 8-17 were deleted. The effect of this modification is to remove all low-level, low-amplitude load transitions in compression, and to permit an acceleration of testing by a factor of about three. Figure 9.40 shows the steady growth of typical impact damage during a test. Conclusions reached as a result of this testing program include the following:

(i) Low-level impact damage can propagate to failure by compression-dominated fatigue under the severe loading spectrum used.

(ii) Damage growth normal to the 0^o fibre direction was pronounced; little growth was evident in the 0^o fibre direction.

(iii) Damage growth rate was in this case controlled by the width of the damaged area, under a simple power-law relationship.

(iv) Load spectrum modification by removal of low load cycles is an acceptable means of accelerating fatigue tests; damage growth is insensitive to the presence of such load cycles.

(v) Variations in material processing can have a significant effect on damage growth. Specifically, omission of a post-cure heat-treatment can reduce fatigue life by a factor of approximately two, while having no significant effect on static strength.

(vi) With careful control of impact damage conditions and test methods, the scatter in fatigue life for composites can be similar to that for metals.

1986/87 Programme (D.S. Saunders - ARL)

Additional fatigue testing of impact-damaged carbon fibre coupons has been undertaken during 1986. The main objective of this work has been to investigate in more detail the process of delamination growth under compression-dominated fatigue loading and to study the damage growth law proposed as a result of earlier work. Although shadow

moire techniques /59, 60/ are still being used to measure delamination size, coupons are now being removed once or twice during the fatigue programme and C-scanned to enable more detailed mapping of damage growth. The results are compared with C-scans of the initial impact damage. Preliminary results obtained using a 5MHz probe suggest that a number of delaminations through the thickness are growing concurrently in the early stages of damage growth. Stiffness measurements are taken throughout the fatigue programme and it is hoped that these can be correlated with damage growth mapped by C-scanning and moire techniques.

Preliminary tests to investigate the effects of a Hot/Wet environment on fatigue life behaviour have been completed. Under the Hot/Wet environment it was found that static strength of impact damaged coupons was reduced to about 85% of the static strength of impact damaged coupons tested under RT/Dry conditions. Peak compressive fatigue loads to give a maximum strain of -2900 με were used for the Hot/Wet fatigue tests. Delaminations were found to grow readily at this strain level, and the scatter in the fatigue-life data was found to be of the same order as that observed for the RT/Dry testing conditions. This work is reported in more detail in /61/.

9.5 FATIGUE LOADS, LIFE MONITORING AND ASSESSMENT

9.5.1 Flight Loads Data (C.T. Stefoulis - DOA)

The Department of Aviation has been actively involved in the field of flight loads data acquisition for General Aviation (GA) aircraft since the mid 1960's. Results from this program have regularly featured in Australian reviews over the past decade as more data became available for analysis. During 1985/86 the majority of accumulated data was analysed by an officer from the Department as part of an overseas postgraduate study program /62/ at the Cranfield Institute of Technology, England. Preliminary results from this analysis are presented and discussed, along with a brief description of the method of analysis.

Over 100,000 hours of fatigue meter (counting accelerometer) data from 49 multi-engined and 8 single-engine aircraft engaged in GA operations throughout Australia and neighbouring Papua New Guinea were analysed. The data were supplemented by records of cruise operating conditions (weights, airspeeds and altitudes), types of aircraft operations undertaken (eg commuter, private or agricultural), aircraft home bases and operating dates. Fatigue meter data were corrected to account for drifts in acceleration recording levels.

The analysis took the direction of comparing the available Australian data with similar data obtained from flight loads surveys conducted over other countries. First, the data were compared with tabulated results from the NASA VGH General Aviation flight loads program, the preliminary results of which were also presented in previous US ICAF reviews. Significant scatter in the cumulative frequency of exceedance for the acceleration spectra was observed for the total combined data (ie all types of operations) in both programs, being around two orders of magnitude (100:1) between the least and most severe individual spectrum.

Following the recommendations of NASA, the Australian and NASA data were categorised according to the type of operation the aircraft was involved in during the program. Scatter was found to generally decrease to around 10:1 for the categorised load spectra, but not to a level which would enable reliable distinctions to be made between various operations. To allow such distinctions to be made, the gust load acceleration spectra were converted to gust velocity spectra using the discrete gust concept with associated aircraft cruise operating conditions. The frequency scatter for the total combined (uncategorised) gust velocity spectra was observed to decrease significantly to around 10:1, with the categorised gust velocity spectra showing even less scatter.

Three main types of operations were investigated; high altitude jet operations, medium altitude executive propeller operations and low altitude survey and aerial application operations. All available data were pooled into one of these three main categories. Second-order polynomials were least squares fitted to the Australian and NASA gust data. These fitted polynomials for the Australian and NASA high altitude jet, medium altitude propeller and low altitude survey operational categories are shown in Fig.9.41. The values of the regression constants are given in Table 9.4. Confidence intervals for the equations were evaluated to account for frequency scatter when comparisons are made between spectra. The spectra for the Australian data are shown in Fig.9.42, and for the NASA data in Fig.9.43.

It was evident from the Australian data in Fig.9.42 that the gust loading severity decreased with increasing altitude. The jet operations showed a decrease of one order of magnitude in the gust velocity loading frequency compared to the survey operation, with the propeller executive operation being around two to three times more severe than the jet operation.

Figure 9.41 indicates that the NASA executive operation negative gust velocity spectrum is similar to the equivalent Australian spectrum for negative gust velocities exceeding 20 ft/sec. Negative gust velocities lower than 20 ft/sec appear to be more frequent for the Australian spectrum by a factor of two over the NASA spectrum. The NASA Survey operation is more severe than the Australian Survey operation for negative gust velocities exceeding 25 ft/sec. This was attributed to the more diverse Survey operations undertaken in the NASA programme. A comparison of the positive gust velocity spectra is not immediately possible due to the influence of positive manoeuvre accelerations on converted positive discrete gust velocities for the Australian data. Fatigue meters cannot discriminate between gust and manoeuvre acceleration inputs, whereas NASA VGH meter data can separate manoeuvre and gust load inputs.

A definite seasonal effect was identified in the Australian data - the gust loading frequency is more severe in summer than in winter. Taking the ±10 ft/sec gust velocity level, the ratio of November/July count rates was 2.50. The seasonal effects and the variation of geographical environment over which the aircraft fly are the main causes for the residual scatter observed in the converted discrete gust velocity spectra. Additional scatter sources were drift in the fatigue meter threshold levels, and possible errors in estimating cruise conditions for the purpose of converting gust accelerations to derived gust velocities.

Finally, a comparison was made of both the Australian and NASA spectra with the corresponding ESDU data /63/. The cumulative gust exceedance spectra required subdivision giving the variation of relative gust frequency with gust velocity for various altitude bands, Figs 9.44 (a) and (b), and the variation of absolute gust frequency with gust velocity and altitude, Fig.9.45. The Australian data are compatible with the ESDU data, although the altitude trend in the ESDU relative gust frequency curves was not so evident in the Australian data. The Australian data appeared to show no marked variation of relative gust velocity frequency with altitude (ie the shape of the relative gust frequency spectra did not significantly change with altitude). The main altitude effect evident in the Australian data is in the variation of absolute gust frequency with altitude, Fig.9.45.

The ratio of upgusts to downgusts is larger for the Australian data than for the ESDU data, this being attributed to the higher manoeuvre content of the smaller GA aircraft compared to the predominantly Transport category source aircraft for the ESDU data. A significant amount of scatter was observed, Fig.9.46, and no general curve could be established to represent any variations with altitude. Insufficient Australian data were available to draw conclusions for the more recreational single-engine operations. From the NASA data, these types of operations tend to show considerable scatter, indicating that further categorisation is warranted. Because of the speed limitations of this class of aircraft, the single- engine aircraft might best be categorised by the geography surrounding the home base.

Variation of pilot experience is also a problem requiring further consideration. The Commuter category identified in the analysis showed the least amount of frequency scatter, which is expected considering the more disciplined approach to commuter flying compared to single-engine aircraft flying.

The major problem with General Aviation flight loads surveys is the large number of individual operations over a significant geographical area. The amount of data sampled in the Australian programme represents less than 0.1% of the total General Aviation operations within Australia. Hence one cannot be sure whether all classes are sampled, and because the programme was operated on a volunteer basis, the question of sample bias towards the "more mature" pilot operations requires further consideration.

Overall, the Australian Flight Load Survey program has successfully sampled enough data to make useful conclusions concerning the severity of the Australian atmospheric gust environment. The program currently remains operational in Australia, although scaled down considerably, and whilst manufacturers continue to produce a wide variety of high technology General Aviation aircraft, the program will still represent a worthwhile Departmental project in fatigue evaluation.

9.5.2 A Thunderstorm Downburst Case Study (D.J. Sherman - ARL)

On 5 November 1977 a weak downburst associated with a multi-cell storm passed over an instrumented tower at Bald Hills, a suburb of Brisbane, Australia. Associated with the thunderstorm was a dome of cold air estimated to be 1200 m to 1800 m deep. Two downdrafts, at least one of which was large enough to be called a down burst, penetrated to the ground near the front edge of this dome. The downburst substantially maintained its vertical velocity down to 100 m above the ground, with one parcel of air having a high vertical velocity and a lateral extent of about 180 m penetrating right down to the 58 m level. At the 100 m level the vertical downdraft had a peak value of 7.5 m/s and its average value was continuously greater than 4 m/s for at least 50 seconds. The ground wind (measured at 10 m) changed from a north wind of 10 m/s to a south wind of 13 m/s in approximately 90 seconds.

Because of restraint by the surrounding flow, the downdrafts did not spread out as a free wall jet, but as a slower, deeper, submerged jet whose thickness was controlled by downstream conditions. About 1 km ahead of the downburst, and within the cold air flowing away from the storm, was a second gust front which may have been the low level manifestation of the ring vortex which initially surrounds a downburst, and is responsible for the severe horizontal outward flow. Just ahead of this second gust front, and centred at a height of about 50 m, was an indication of a counter-rotating vortex which suggests that the boundary layer of the cold outflow may have separated from the ground, causing the initial ring vortex to lift and so reduce the horizontal outflow wind speeds at ground level.

The study is fully reported in /64/.

9.5.3 Fatigue Monitoring of RAAF Aircraft (P.J. Foden - HDHV)

9.5.3.1 DADTA on RAAF Macchi MB326H Aircraft

Hawker de Havilland (Victoria) is carrying out a durability and damage tolerance programme for the RAAF on its Macchi MB 326H fleet. The project began with a review of the literature, and an analytical crack growth programme which was developed from work which the company had done for the RAAF Mirage fleet. The results of this preliminary phase were used to assess the relative sensitivity of the large number of control points initially selected.

In the second phase, the more critical points are being investigated in greater detail, some by analysis and some by test. Aircraft components removed during the LOTEX programme are being used in the test programme where they represent the current configuration. In addition, material removed from the aircraft at LOTEX (e.g. spar caps and fuselage longerons) has been used to manufacture coupons. These are being used to derive da/dN data which is used in the crack growth analysis programme.

All results will finally be drawn together in an ASIP exercise, the aim of which is to allow the fleet to continue in service, with no reduction in safety margin.

9.5.3.2 F/A-18 Fatigue Monitoring

HDHV has implemented a Maintenance Data and Service Life Monitoring System (MD&SLMS) for the airframe and engine of the RAAF F/A-18. The system collects and analyses flight parameters and airframe strain data recorded by the on-board Maintenance Signal Data Recording Set (MSDRS) supplied by the manufacturer (McDonnell Douglas). In addition, a 12-channel Aircraft Fatigue Data Analysis System (AFDAS Mk III - manufactured by British Aerospace, Australia) is fitted to RAAF F/A-18s. AFDAS enables a broader coverage of the airframe to be monitored at a higher frequency response than is otherwise available. Strain data are recorded in time sequences for MSDRS and for individual flights by AFDAS. The total MD&SLMS system consists of dedicated DEC VAX computers for each operating squadron, deployable micro-VAX systems and a central computer at HDHV which analyses the longer term life information using the ORACLE relational database management system. Airframe fatigue calculations are based on McDonnell Douglas SAFE software although other methodologies may be used in the future. Information from the system is also used to life engine parts as well as in helping to diagnose faults in unservicable operating squadron aircraft.

9.5.3.3 F-111 Aircraft Monitoring

It was reported in the previous Review /1/ that the RAAF intends to monitor each individual F-111 aircraft using the Aircraft Fatigue Data Analysis System (AFDAS). A prototype fitting of AFDAS equipment to one F-111 aircraft was completed during 1985, and data from this aircraft are currently being acquired from 17 strain gauge locations. Detailed analysis is to begin shortly.

Drawings are being prepared for the fitting of AFDAS units to most of the RAAF F-111 fleet. Each unit will monitor the output of eleven strain gauges rather than the 17 used for the prototype installation.

9.5.3.4 Mirage Aircraft Monitoring

The RAAF Mirage was the first aircraft type to be fitted with AFDAS equipment. Some difficulties encountered in this departure from more traditional loads monitoring procedures have been overcome and the extension of AFDAS installation to other RAAF aircraft types is proceeding in a comparatively routine manner. Since the Australian Mirage fleet is now being phased out, Mirage AFDAS monitoring has been discontinued. Individual aircraft tracking is nevertheless being continued using fatigue meter data in conjunction with computer-based flight-by-flight crack growth models developed by HDHV which were based directly on AFDAS data generated by the fleet.

9.5.3.5 Macchi MB326H Aircraft Monitoring

Individual RAAF Macchi MB326H aircraft monitoring is continuing using fatigue meter data. One aircraft has been AFDAS-fitted and plans for fitting AFDAS to a further ten aircraft are underway. Monitoring locations on the Macchi include the wings, wing carry-through structure, fin and horizontal tail support structure.

9.5.3.6 Nomad Aircraft Monitoring

HDHV is currently preparing drawings for the fitting of AFDAS equipment to one aircraft. Once this has been demonstrated as satisfactory, AFDAS will be fitted to a small sample of the fleet. In conjunction with GAF, the designers of the Nomad, seven strain gauge locations have been selected. These cover the main wing, wing struts, stub wing, fin and tailplane.

9.5.3.7 C-130 Aircraft Monitoring

HDHV is currently developing a proposal for software to automate the tracking of individual RAAF C130E and C130H aircraft usage within defined mission categories. This information is to be used by the RAAF to monitor more conveniently the fatigue status of each aircraft.

9.6 BIBLIOGRAPHY ON THE FATIGUE OF MATERIALS, COMPONENTS AND STRUCTURES (J.Y. Mann - ARL)

The fourth volume of this work by J.Y. Mann will now cover the period 1966 to 1969 instead of 1966 to 1970 because of the large number of citations found in the four-year period and difficulties experienced in their verification. Volume 4 is currently being entered into a small computer, and is now expected to be published during 1987. (Volumes 1, 2 and 3 of the Bibliography covering the periods 1838-1950, 1951-1960 and 1961-1965 were published by Pergamon Press in 1970, 1978 and 1983 respectively.)

9.7 REFERENCES

1. Jost, G.S. A review of Australian investigations on aeronautical fatigue during the period April 1983 to March 1985. Minutes of the 19th ICAF Conference, Pisa, May 1985.

2. Higgs, M.G.J. Mirage A3-002 Strain Responses to Ground Calibration Loadings Between 1978 and 1985. ARL Structures Tech Memo 425, December 1985.

3. Grandage, J.M. Ground Calibration Data for Columbia Gauges Fitted to Mirage IIIO, ARL Structures Tech Memo 428, January 1986.

4. Grandage, J.M. Report on Mirage Tripartite Meeting held in December 1986, ARL Structures Tech Memo (in publication).

5. Parker, R.G. CT4 Air Trainer Full Scale Fatigue Test. ARL Structures Tech Memo (in publication).

6. Gratzer, L.R. The Test Load Sequences applied to the CT4 Full Scale Fatigue Test. ARL Structures Tech Memo 416, May 1985.

7. Gratzer, L.R. The CT4 Flight Trials Programme. ARL Structures Tech Memo 449, August 1986.

8. Tuller, L.T. A Summary of critical fatigue lives and inspection requirements. GAF Nomad Project Note N2/110, September 1985.

9. Romeyn, A. Wing spar cracking - Rockwell 112B, 114. Lab Note 591, Materials Evaluation Facility, Department of Aviation, Canberra, November 1986.

10. Romeyn, A. Grumman G-164 Aileron Interconnect Strut Failure, VH-SLK. Specialist Report No X-30/84, Materials Evaluation Facility, Department of Aviation, Canberra, January 1985.

11. Romeyn, A. Examination of Cracking in a Bell 205 Main Rotor Blade. Specialist Report X-9/86, Materials Evaluation Facility, Department of Aviation, Canberra, August 1986.

12. Romeyn, A and Hollamby, D.C. Investigation of Fatigue Cracking in Bell 47 Main Rotor Grips. Specialist Report No. X-10/85. Materials Evaluation Facility, Department of Aviation, Canberra, September 1985.

13. Romeyn, A. Vertical Stabiliser Attachment Brackets, Robinson R22 VH-LCH. Lab Note 593, Materials Evaluation Facility, Department of Aviation, Canberra, November 1986.

14. Beaver, P.W.; Mann, J.Y.; Sparrow, J.G. A grid technique for the measurement of strains close to cold-expanded holes. Measurement and fatigue - EIS-86. Bournemouth, England, March 1986, pp. 491-505.

15. Beaver, P.W.; Mann, J.Y.; Sparrow, J.G. Fatigue life enhancement by the cold-expansion of holes - research and case study. Fatigue prevention and design. Amsterdam, The Netherlands, April 1986.

16. Mann, J.Y.; Sparrow, J.G.; Beaver, P.W. Cold expansion of holes to extend the fatigue lives of structures. 10th Australasian Conference on the mechanics of structures and materials. Adelaide, Australia, August 1986, pp. 93-99.

17. Mann, J.Y.; Machin, A.S.; Lupson, W.F. Improving the fatigue life of the Mirage IIIO wing main spar. ARL Structures Report No. 398, January 1984.

18. Carey, R.P. and Hoskin, B.C. A finite element procedure for interference-fit and cold-working problems with limited yielding. ARL Structures Report No. 425, December 1986.

19. Steven, G.P. and Care, G. Non-linear finite element analysis of a large plate containing a cold expanded hole. University of Sydney, Department of Aeronautical Engineering Technical Report, January 1986.

20. Steven, G.P. Cyclic loading and 3-D FEA of cold-worked holes. University of Sydney, Department of Aeronautical Engineering Report (in preparation), 1987.

21. Heller, M. Jones, R. and Williams, J.F. Analysis of bonded inserts for the repair of fastener holes. Eng. Frac. Mechanics, 24(4), 523-532, 1986.

22. Machin, A.S. and Sparrow, J.G. The SPATE 8000 Thermoelastic stress analyser. Non-Destructive Testing Australia 23(4), 1986, pp. 96-100.

23. Machin, A.S. and Foden P. A stress survey of a Wamira tailplane spar using the SPATE 8000 stress analyser. ARL Structures Tech Memo 434, March 1986.

24. Machin, A.S. and Watters, K.C. Thermoelastic inspection of a wing main spar lower attachment fitting. ARL Structures Tech Memo in preparation.

25. Machin, A.S., Sparrow, J.G. and Stimson, M.G. Mean stress dependance of the thermoelastic constant. To be published in STRAIN, February 1987.

26. Machin, A.S., Sparrow, J.G. and Stimson M.G. The thermoelastic constant. Paper presented to Second International Conference on Stress Analysis by Thermoelastic Techniques. London, February 1987.

27. Wong, A.K., Jones, R. and Sparrow, J.G. Thermoelastic constant or thermoelastic parameter? Paper submitted to Journal of Physics and Chemistry of Solids, December 1986.

28. Rumble, S.J. and Sparrow, J.G. Determination of the dependence of ultrasonic shear wave transit times on temperature, stress and frequency. ARL Structures Tech Memo 405, March 1985.

29. Rumble, S.J. and Sparrow J.G. Ultrasonic transit time measurements using fast analogue to digital conversion and a fast Fourier transform based algorithm. ARL Structures Tech Memo 406, March 1985.

30. Rumble, S.J. and Sparrow, J.G. Review of ultrasonic velocity methods of determining residual stress. ARL Structures Tech Memo 416, May 1985.

31. Watters, K.C., Sparrow, J.G. and Jones R. Shadow moire monitoring of damaged graphite/epoxy specimens. ARL Structures Tech Memo 398, February 1985.

32. P'cruz, J., Lawrie, B.L., Watters, K.C. and Rumble, S.J. Experimental aspects of in-plane displacement measurement using a moire fringe technique. ARL Structures Tech Memo 440, June 1986.

33. Lawrie, B.L. Preliminary study of holographic interferometry applied to carbon fibre specimens. ARL Structures Tech Memo 419, August 1985.

34. Heller, M. and Rumble, S.J. Vibration analysis of a CFRP plate. ARL Structures Tech Memo 438, May 1986.

35. Rumble, S.J. and Lawrie, B.L. Preliminary investigation of the use of holographic interferometry to detect ill-fitting compressor blades. ARL Structures Tech Memo 451, November 1986.

36. Rumble, S.J. Introduction to holographic interferometry applied to strain determination in aircraft structures. ARL Structures Tech Memo 443, June 1986.

37. Beaver, P.W. An evaluation of microgridding techniques for determining local plastic strain distributions. ARL Structures Tech Memo 454, November 1986.

38. Beaver, P.W. A microgridding and replicating technique for measuring local plastic strain distributions under static and cyclic loading. Proc. 1985 Symposium of the Australian Fracture Group, B.L. Karihaloo (Ed.), University of Sydney, 1985, pp. 12-21.

39. Beaver, P.W., Heller, M. and Rose, T.V. Experimental and theoretical determination of J_{IC} for aluminium alloy 2024-T351. ARL Structures Report 420, July 1986. (Submitted to Fatigue and Fracture of Engineering Materials and Structures.)

40. Beaver, P.W. J - integral testing of aluminium alloys - a new technique for marking crack fronts. ARL Structures Tech Memo 439, June 1986. (Submitted to Journal of Testing and Evaluation.)

41. Beaver, P.W. The effects of crack tip plastic strain distribution on fatigue crack growth in high strength aluminium alloys. Proc. 1986 Materials Technology Congress, Vol. 2, Institution for Metals and Materials Australasia Ltd., Adelaide, 3-A-2, 1986, pp 1-10.

42. Beaver, P.W. Multiaxial fatigue and fracture - a literature review. ARL Structures Report 410, 1984.

43. Beaver, P.W. Biaxial fatigue and fracture of metals - a review. Metals Forum, 8(1), 1985, pp. 14-29.

44. Beaver, P.W. A review of multiaxial fatigue and fracture of fibre-reinforced composites. ARL Structures Report (in publication).

45. Finney, J.M. & Machin, A.S. Symposium of Australian Fracture Group, University of Sydney, Nov. 1985, pp. 85-94.

46. Finney, J.M. & Denton, A.D. Cycle counting and reconstitution, with application to the aircraft fatigue data analysis system. Int. Conf. on Fatigue of Engineering Materials and Structures, Univ. of Sheffield (Proc. Inst. Mech. Engrs) vol 1, Sept 1986, pp 231-240.

47. Ford D.G., Fatigue Life Distribution for Structures with Interacting Failures. Probabilistic Methods in the Mechanics of Solids and Structures. Editors S. Eggwertz & N.C. Lind, Springer-Verlag 1985. (Proc. IUTAM Symposium, Stockholm 19-21 June 1984.)

48. Cramer, H. and Leadbetter, M.R. Stationary and Related Stochastic Processes, Wiley 1967.

49. Piperias, P. and Ford, D.G. A program for the determination of the second up-crossing density in stationary gaussian processes. ARL Structures Report (in preparation), 1987.

50. Ford, D.G. Range-mean-pair exceedances from stationary, normal, random processes. Paper No 13 presented to the first IFIP Working Conference held at Aalborg, May 6-8, 1987.

51. Baker A.A. Fibre Composite Repair of Cracked Metallic Structure. Proceedings of AGARD Conf. The Repair of Aircraft Structures Involving Composites, Norway, April 1986.

52. Jost, G.S. A review of Australian investigations on aeronautical fatigue during the period April 1981 to March 1983. Minutes of the 18th Conference of the ICAF, Toulouse, May 30-31, 1983.

53. Ilic, S. and Williams. J.F. Compression failure modes in composites. Theor & App. Frac. Mech., 6, (12), 121-128, 1986.

54. Ilic, S., Williams, J.F. and Jones, R. Instability related delamination growth. Proc. Conf. of the Australian Fracture Group, Sydney, 1986, pp.95-104.

55. Williams, J.F., Stouffer, D.C., Ilic, S. and Jones, R. An analysis of delamination behaviour. Int. J. Composite Structures, 5, 203-216, 1986.

56. Scala, C.M. A semi-adaptive approach to in-flight monitoring using AE. Presented at Review of Progress in Quantitative NDE, San Diego, August 1986.

57. Scott, I.G., Scala, C.M. An overview of Australian research in NDT. Presented at Conference on NDT & E of Advanced Materials and Components, Colorado Springs, August 1986.

58. Preuss, T.E. Ultrasonic depth C-scanning of carbon fibre composite coupons. ARL Tech Memorandum in preparation.

59. Clark, G. and van Blaricum, T.J. Carbon fibre composite coupons - static and fatigue behaviour after impact damage. ARL Structures Report in preparation.

60. Clark, G. and van Blaricum, T.J. Load spectrum modification effects on fatigue of impact-damaged carbon fibre composite coupons. Composites, (in press).

61. van Blaricum, T.J. Saunders, D.S. and Clark, G. Damage tolerance of impact damaged carbon fibre composite wing skin laminates. Paper 3.3, 14th ICAF Symposium, Ottawa, June 1987.

62. Stefoulis, C.T. An evaluation of measured Australian Gust Data. Cranfield Institute of Technology, College of Aeronautics, MSc Thesis 1985/86.

63. ESDU Data Item 69023. Average gust frequencies (for) subsonic transport aircraft. Engineering Sciences Data Unit, September 1969.

64. Sherman, D.J. The Bald Hills downburst: a thunderstorm downburst case study. To be published in Swiss Aero Review, 1987.

APPENDIX

N.D.I. PROCEDURE DOA/NDI/EC6

THE EDDY CURRENT INSPECTION OF BELL47 MAIN ROTOR GRIPS

1. **Purpose of the Inspection**

The purpose of this inspection is to detect the presence of fatigue cracking in the root of the internal thread in the inboard end of BELL 47 Main Rotor Grips as required by Airworthiness Directive AD/BELL47/92.

2. **Preparation Required**

The threaded section of the Grip must be clean and free from any foreign matter which may cause the probe to tilt as it is scanned around the thread.

3. **Equipment Required**

3.1 A suitable eddy current flaw detector. This procedure was constructed using the Locator UH instrument manufactured by Hocking Electronics.

3.2 A special eddy current probe shaped to fit the thread and containing a coil position so that its ferrite core is contiguous with the root of the thread.

3.3 A standard aluminium test block containing a 0.5mm (0.020") deep slot not more than 0.25mm (0.010") wide.

3.4 A turntable with a fixture to support a Grip with its threaded end uppermost. (This is not essential but will greatly assist in scanning the probe during the inspection.)

Note 1: Other test equipment operating in the medium frequency range (100KHz-500KHz) may be used subject to the approval of the Department.

Note 2: Special probes suitable for use with a Locator UH instrument are available through Regional Offices of the Department. To assist those who may wish to manufacture probes for use with other instruments, perspex sections moulded to fit the thread may also be obtained through Regional Offices.

4. **Procedure Using the Locator UK Instrument**

4.1 Switch on the instrument and adjust the frequency selector to 500KHz and the material selector to "Al.Mg."

4.2 Place the probe on the standard test block with the coil positioned remote from the slot. Press the "train" button and observe that the lower LED is illuminated. Adjust for lift-off by rocking the probe to illuminate each LED in turn until both are extinguished. At this point rocking the probe should result in negligible movement of the meter needle.

4.3 Press the "zero" button and traverse the probe over the 0.5mm deep slot. Adjust the sensitivity control so that the maximum needle deflection produced by the slot equals 50 divisions.

4.4 Place the prove in the threaded section of the Grip to be inspected so that the coil is positioned in the fourth or fifth thread from the top (inboard end). Press the "train" button and readjust for lift-off as described in 4.2. Press the "zero" button and traverse the probe around the thread in a clockwise direction to inspect the entire thread to its outboard run-out.

4.5 Any crack-like indication resulting in a meter deflection of 50 divisions or greater is cause for rejecting the Grip. Crack-like indications are characterised by a relatively fast needle deflection at the extrmeities of the indication. These must be distinguished from any conductivity changes in the forging which will be characterised by slow, steady needle deflections which are repeatedly obtained as the probe traverses past similar areas of the forging.

5. **Procedure for other Instruments**

If instruments other than the Locator UH are to be used, a written procedure based on that given in 4 above must be prepared and submitted, together with a sample of the probe to be used, to the Department for approval.

TABLE 9.1

SUMMARY OF SEVERED FRAMES IN SECTION 41

REPORTED ON QANTAS 747 AIRCRAFT

FUSELAGE BODY STATION	NUMBER OF REPORTED OCCURRENCES	TOTAL TIME IN SERVICE WHEN SEVERED FRAMES WERE DETECTED (FLIGHT CYCLES)
240	2	10591, 11435
300	6	10025, 10490, 10529, 10591, 10705
320	5	10025, 10490, 10529, 10591
360	1	10490
400	1	11435
420	1	10705
500	1	11435

TABLE 9.2

J_{IC} VALUES DETERMINED BY VARIOUS METHODS

Method	Specimen Number	Stress State	J_{IC} (kJ/m^2)	95% Confidence Interval (kJ/m^2)
(a) Experimental				
Multiple specimen test	-	plane strain	16.9	12.1-21.7
Crack tip strain profile method	BP22	plane stress	≥ 20.0	13.8-26.2
	BP27	"	21.8	16.2-27.4
	BP22	plane strain*	≥ 18.0	12.4-23.6
	BP27	"	19.6	14.6-24.7
(b) Numerical				
FEM hybrid contour method	BP22	plane strain	17.8	14.5-26.1
	BP27	"	22.5	
Modified LEFM approach	BP22	plane strain	18.1	
	BP27	"	22.5	

* Estimates of the plane strain J_{IC} values were obtained from the plane stress values using the following equation:

$$J_{IC} \text{ (plane strain)} = (1 - \nu^2)\, J_{IC} \text{ (plane stress)}$$

where ν is Poisson's ratio and has the value of 0.31 for aluminium alloy 2024-T351.

TABLE 9.3

COMPARISONS OF CRACK GROWTH LIVES

Comparison	Stress Scale MPa/g	Crack growth model *				Exptl.
		Un	Wh	MW	Wi	
f-b-f/Random	11.0	99	98	101	95	106
(%)	17.0	101	100	97	99	105
Accel./Retard.	11.0	102	109	107	115	104
(%)	17.0	98	119	103	98	116
Accel./Random	11.0	87	82	75	66	159
(%)	17.0	91	75	65	65	151

* Un : Unretarded
Wh : Wheeler
MW : Modified Willenborg
Wi : Willenborg

TABLE 9.4

GUST SPECTRA REGRESSION COEFFICIENTS

GUST SPECTRUM	a	b	c
Australian Twin Engine Executive Spectrum -			
Positive	2.7640	-0.2147	0.001741
Negative	2.6865	0.2543	0.002784
Australian Survey Operations -			
Positive	2.8169	-0.1824	0.001457
Negative	2.4936	0.1824	0.001387
Australian Jet Operations -			
Positive	2.5977	-0.2485	0.002775
Negative	2.4301	0.2823	0.003541
NASA Twin Engine Executive Spectrum -			
Positive	2.1103	-0.2114	0.002286
Negative	1.9684	0.2066	0.002078
NASA Survey Operations -			
Positive	2.2128	-0.1799	0.001953
Negative	2.1311	0.1753	0.001925

$$y = a + bx + cx^2$$

where

$y = \log_{10}$ (cumulative frequency of gust exceedance)

x = derived gust velocity (ft/sec)

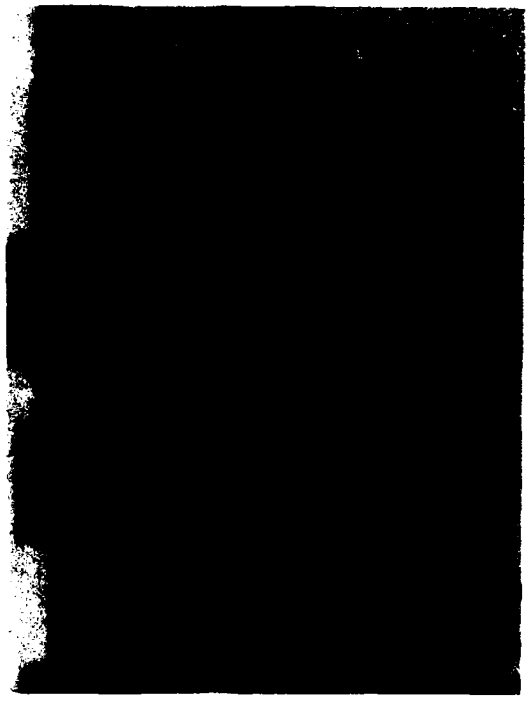

FIG.9.1 SECOND NOMAD STUB-WING UPPER SPAR CAP FAILURE AT BL47.6

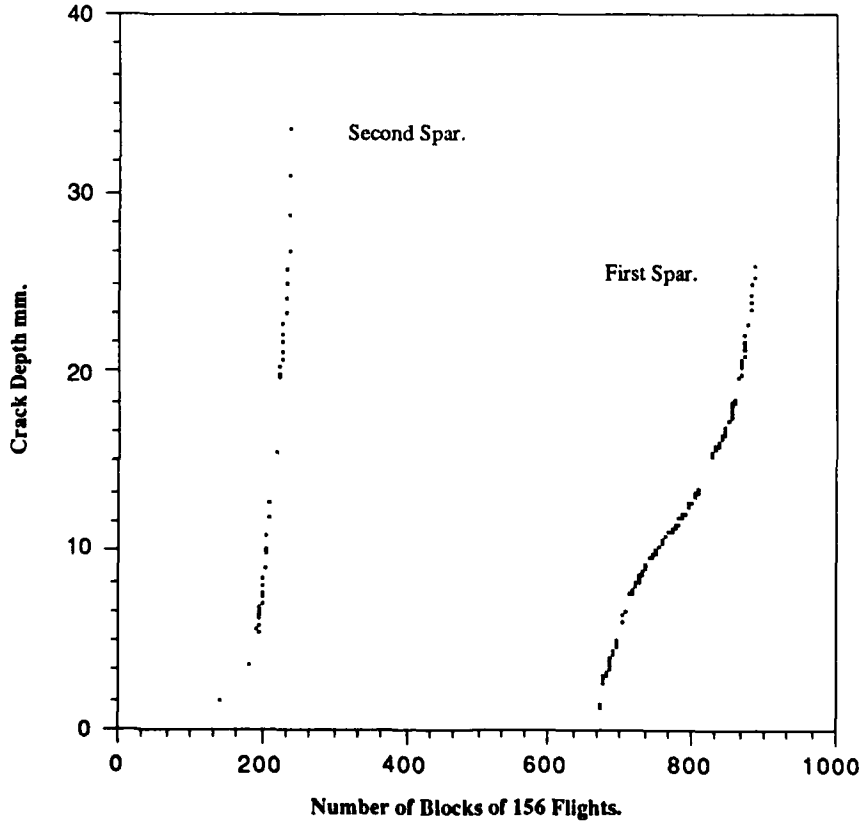

FIG.9.2 FATIGUE BEHAVIOUR OF FIRST AND SECOND NOMAD STUB-WING FAILURES AT BL 47.6

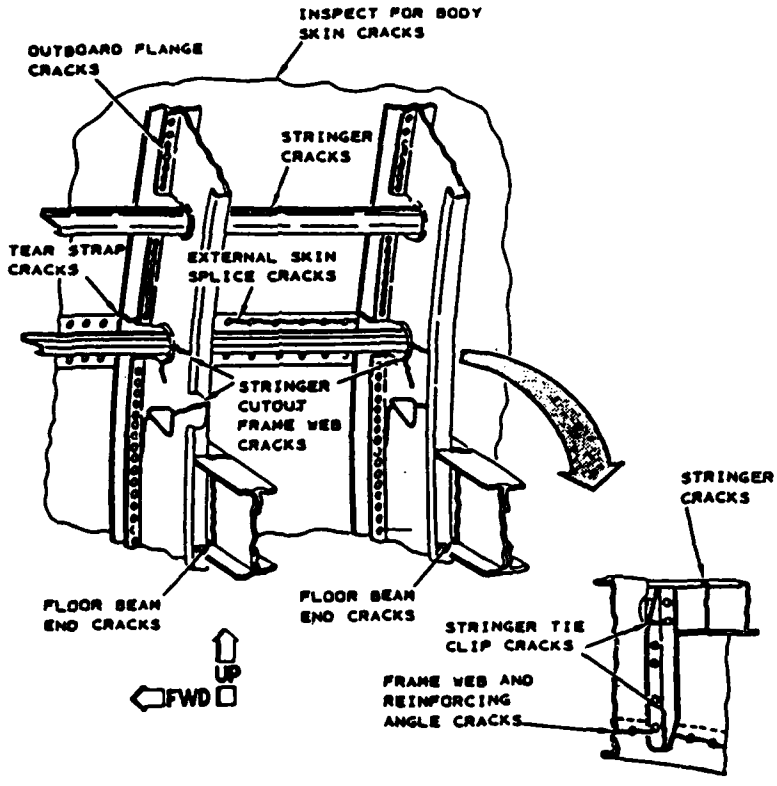

FIG.9.3 TYPICAL CRACKING IN BOEING 747 FORWARD FUSELAGE

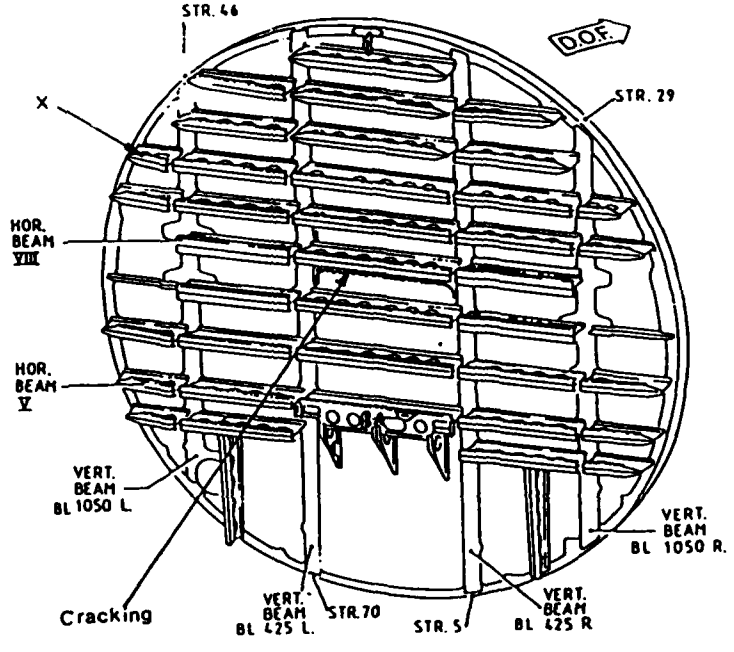

FIG.9.4 FOKKER F28 REAR PRESSURE BULKHEAD SHOWING CRACKING LOCATION ON AIRCRAFT SUFFERING DECOMPRESSION IN FLIGHT

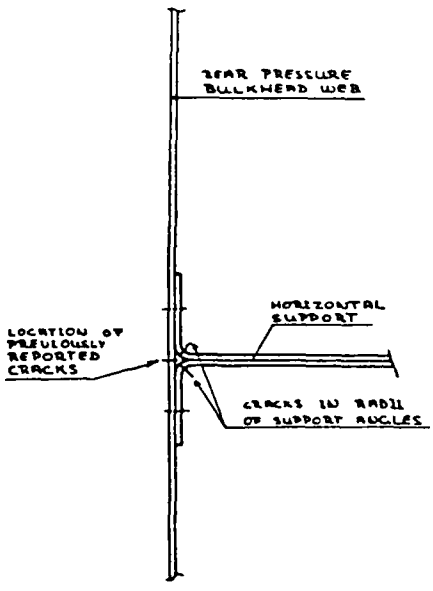

FIG.9.5 TYPICAL LOCATIONS OF F28 BULKHEAD CRACKS

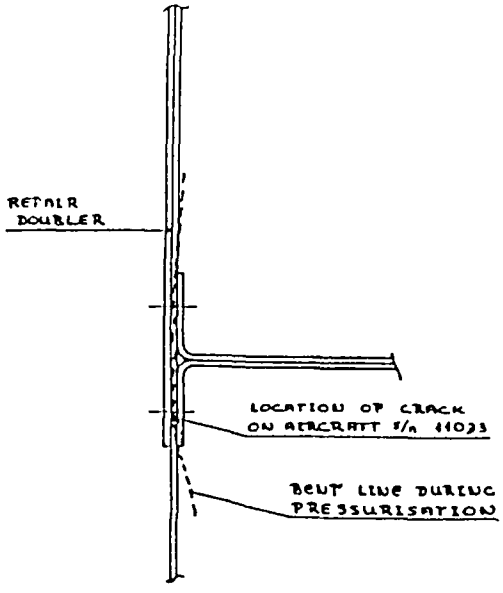

FIG.9.7 CROSS SECTION OF DOUBLER INSTALLATION ON F28 BULKHEAD

FIG.9.6 SECTION OF F28 BULKHEAD WEB SHOWING CRACKED EDGE (TOP) AND ADDITIONAL CRACKING (ARROWED)

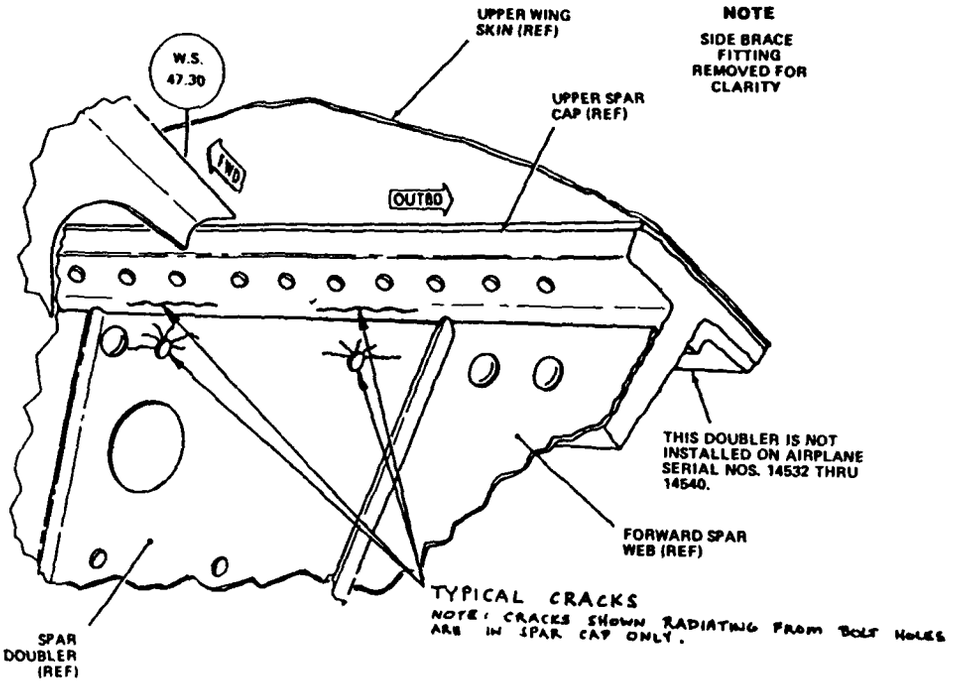

FIG.9.8 GULFSTREAM 112/114 FORWARD UPPER SPAR CAP SHOWING LOCATION OF CRACKING

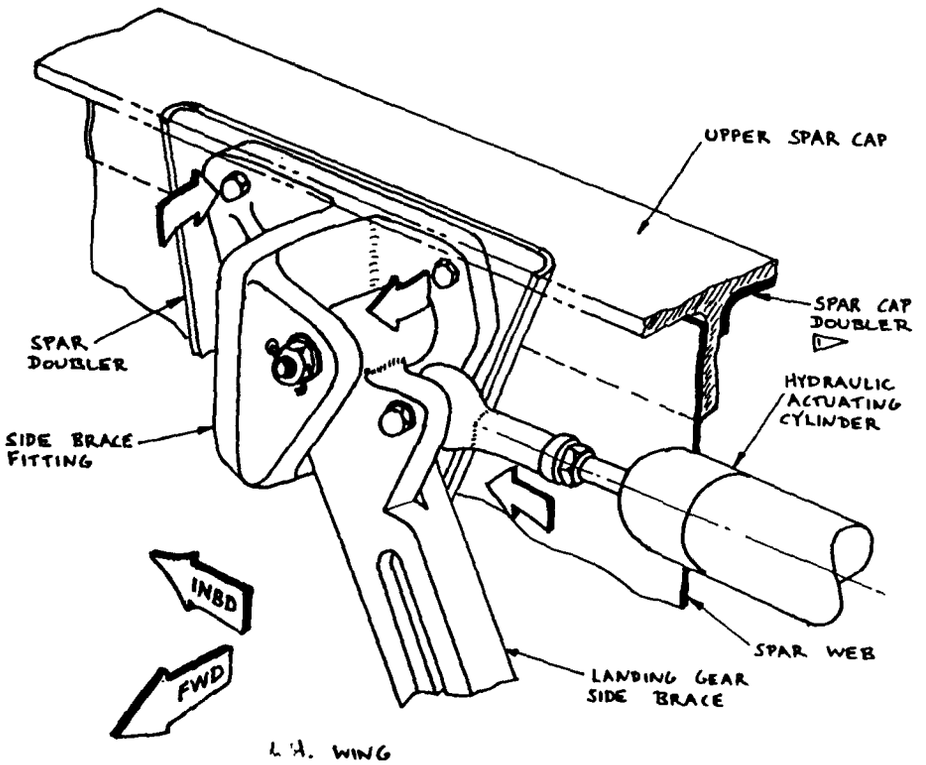

FIG.9.9 GULFSTREAM 112/114 MAIN LANDING GEAR SIDE BRACE FITTING SHOWING OUT-OF-PLANE BENDING LOADS APPLIED DURING GEAR RETRACTION

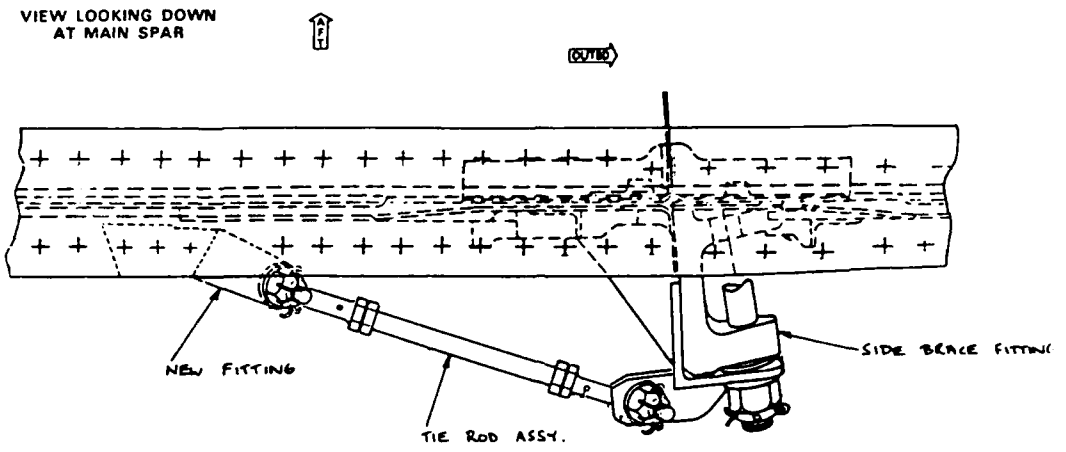

FIG.9.10 GULFSTREAM 112/114 SIDE BRACE FITTING STABILISER

FIG.9.12 BELL 205 MAIN ROTOR BLADE FATIGUE CRACK SURFACE (AFTER SECTIONING)

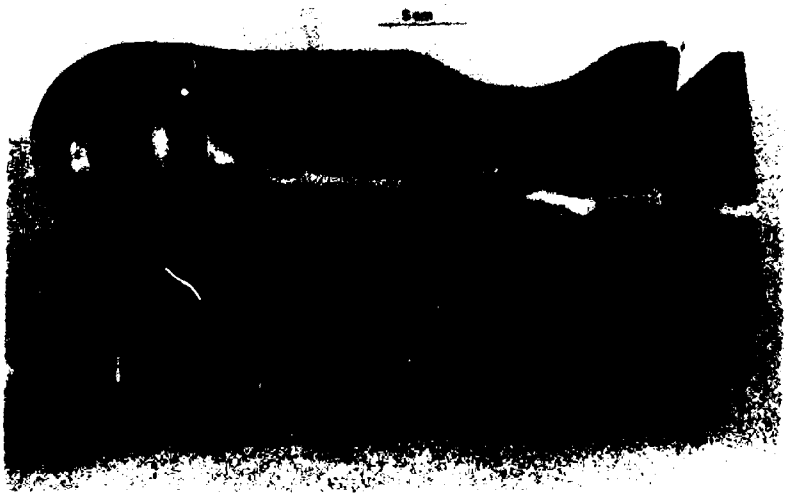

FIG.9.13 BELL 47 MAIN ROTOR BLADE GRIP FATIGUE FAILURE

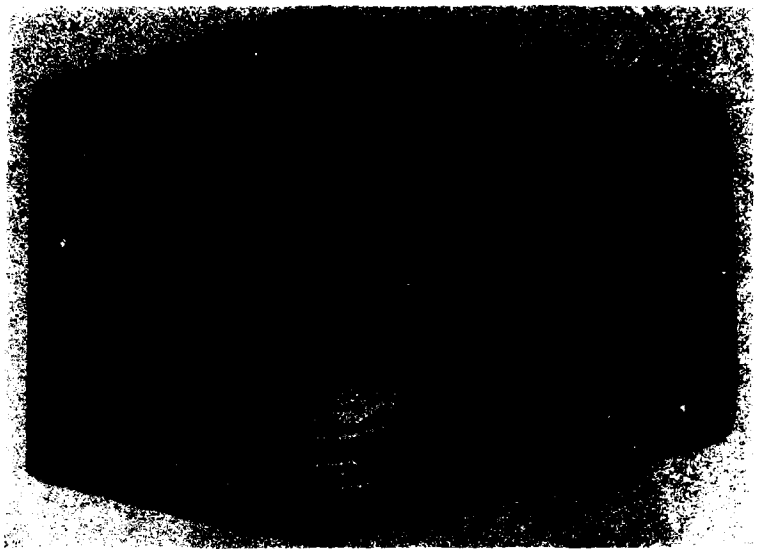

FIG.9.14 BELL 47 MAIN ROTOR BLADE GRIP FRACTURE SURFACE

FIG.9.15 BELL 47 MAIN ROTOR BLADE GRIP FAILURE - SEM OF FRACTURE SURFACE (x 450)

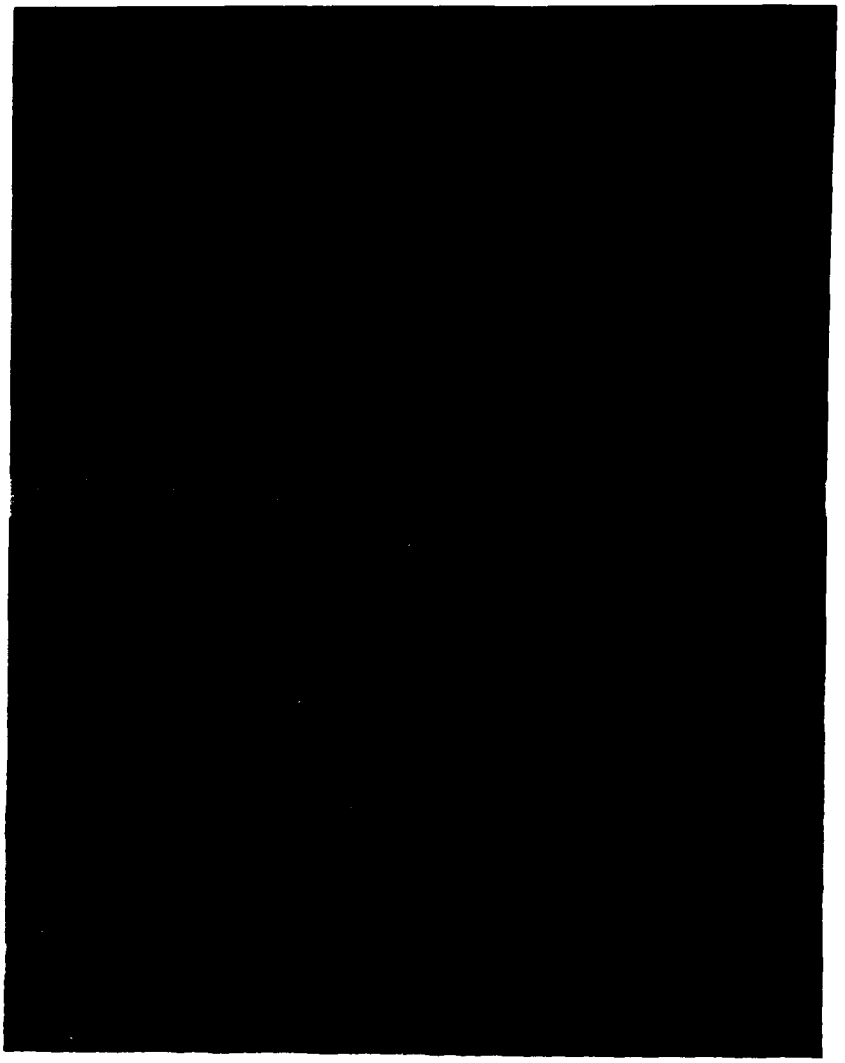

(a) x 6.2

(b) x 30

FIG.9.16 BELL 47 MAIN ROTOR BLADE GRIP - MICROGRAPHS FROM SECOND GRIP OF ACCIDENT AIRCRAFT

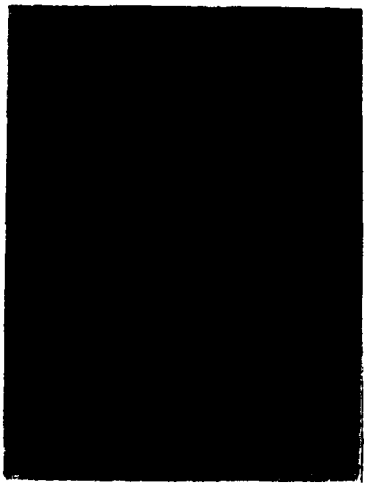

FIG.9.17 EDDY CURRENT PROBE FOR BELL 47 MAIN ROTOR BLADE GRIP

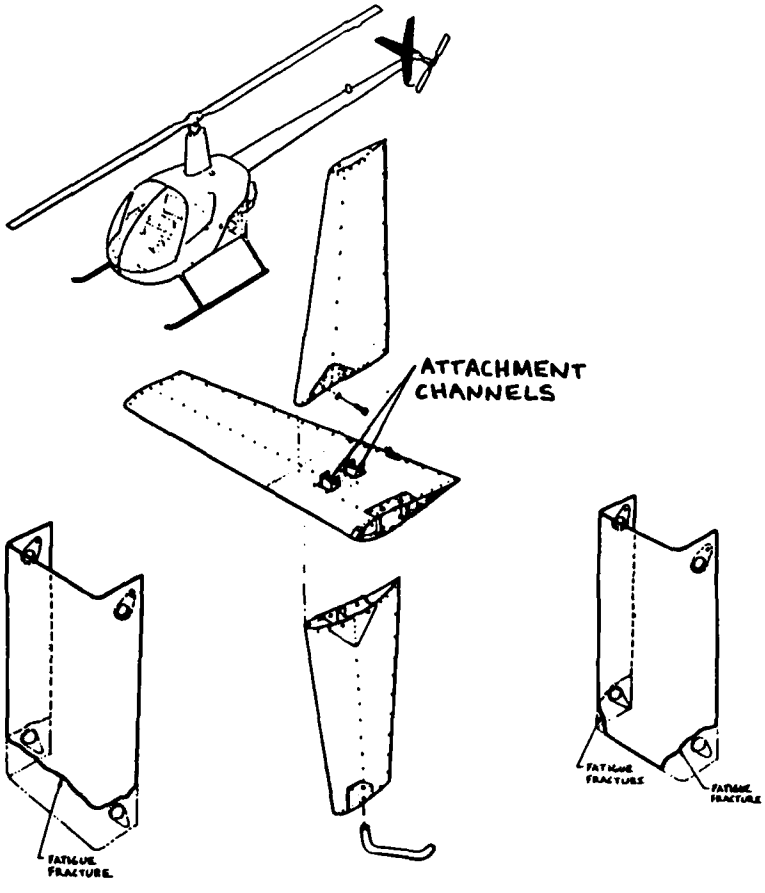

FIG.9.18 ROBINSON R22 FIN ATTACHMENT CHANNEL CRACKING

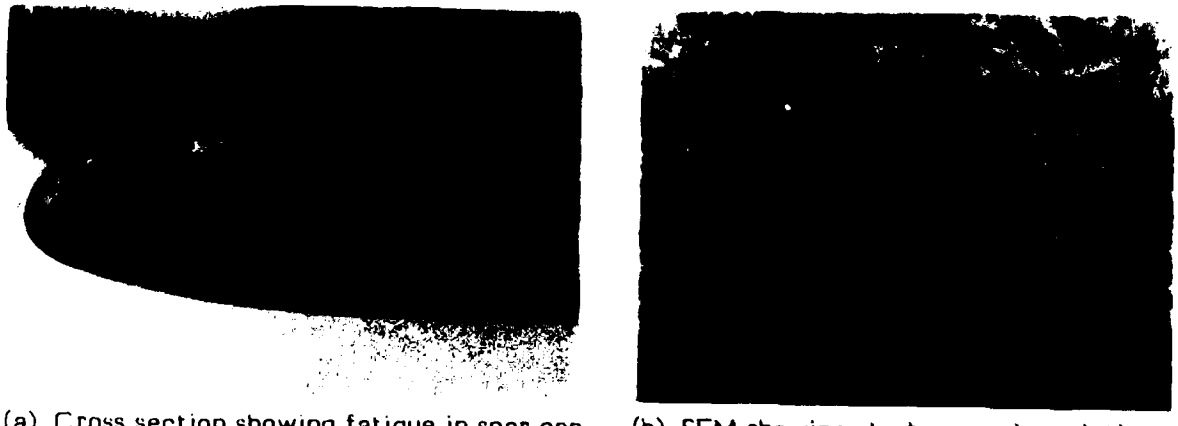

(a) Cross section showing fatigue in spar cap (b) SEM showing start-up cycle striations

FIG.9.19 SA330J PUMA TAIL ROTOR BLADE FAILURE

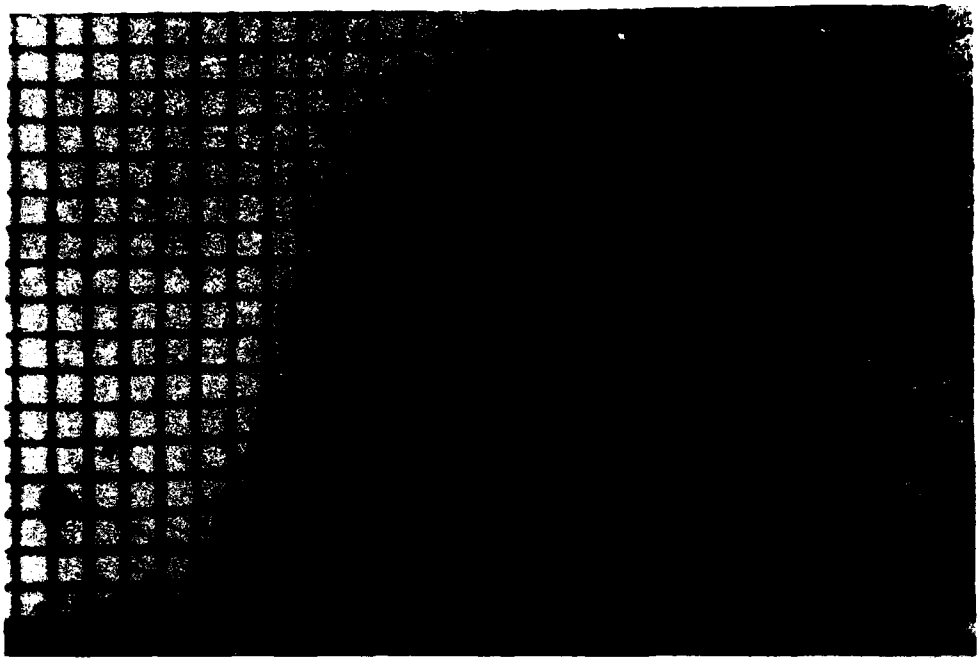

FIG.9.20 SPLIT-SLEEVE COLD-EXPANSION - DEFORMATION ASSOCIATED WITH SPLIT (50 MICRON GRID)

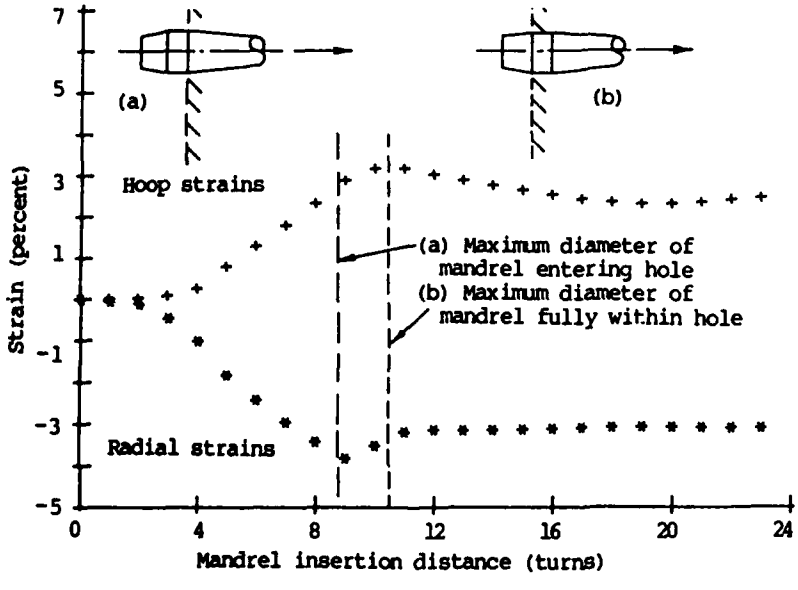

FIG.9.21 SPLIT-SLEEVE COLD-EXPANSION - STRAINS AT HOLE DURING PROGRESSIVE MANDREL INSERTION (STRAIN GAUGE DATA)

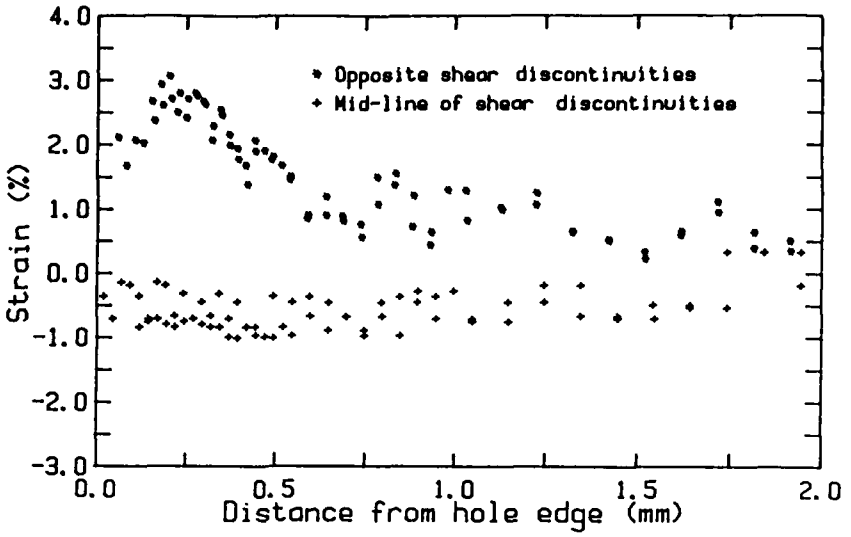

(a) Inlet face

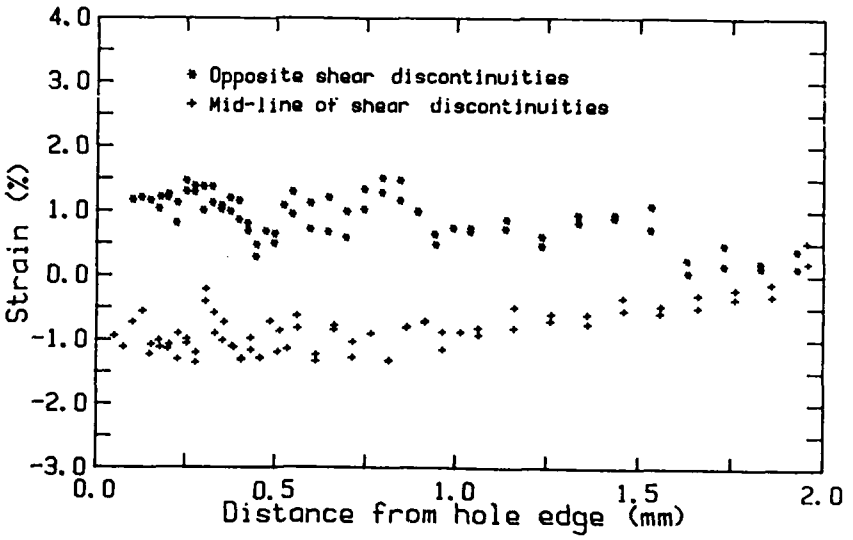

(b) Outlet face

FIG.9.22 SPLIT-SLEEVE COLD-EXPANSION - HOOP STRAINS ON MANDREL INLET AND OUTLET FACES (MICROGRID DATA)

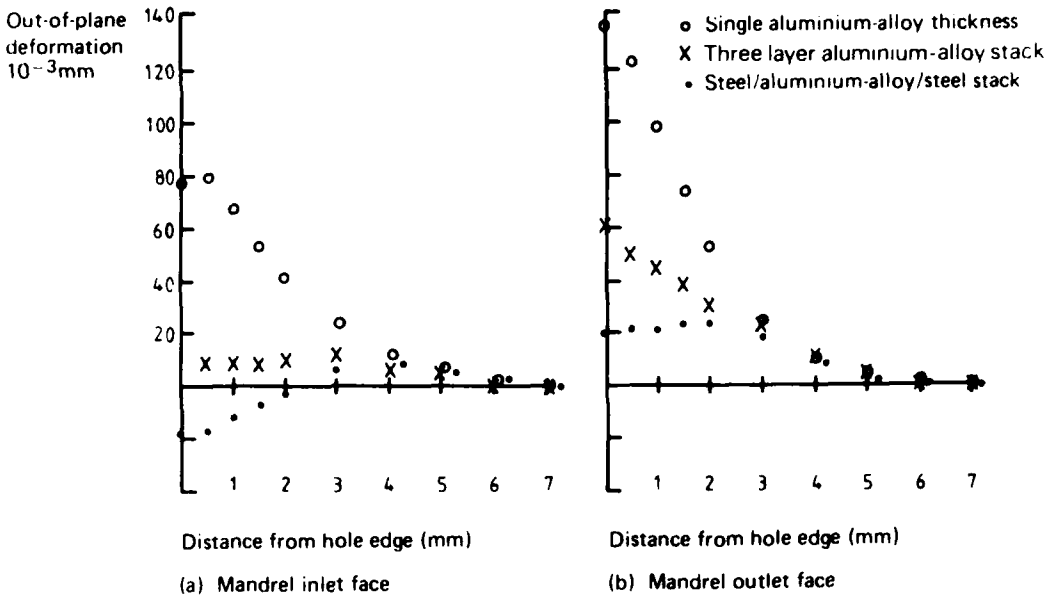

FIG.9.23 SPLIT-SLEEVE COLD-EXPANSION - OUT-OF-PLANE DISPLACEMENT

FIG.9.24 SPLIT-SLEEVE COLD-EXPANSION - TYPICAL FRACTURE SURFACE FOR THICK SPECIMENS (A7-U4SG ALUMINIUM ALLOY, 23 MM THICK) MANDREL INLET FACE AT TOP

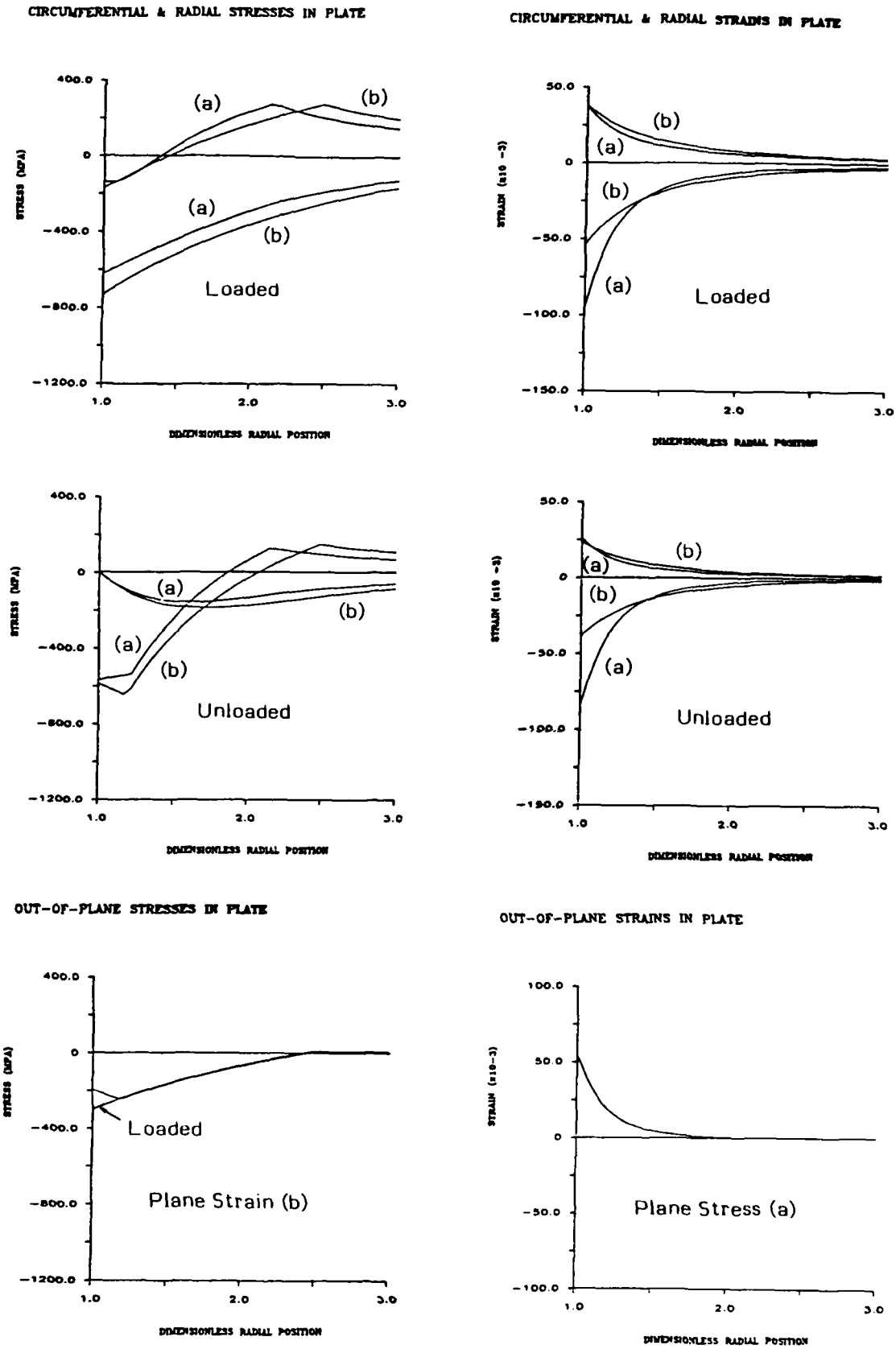

FIG.9.25 NUMERICAL ANALYSIS OF STRESS AND STRAIN AROUND 4% COLD-EXPANDED HOLE IN A LARGE ALUMINIUM ALLOY PLATE

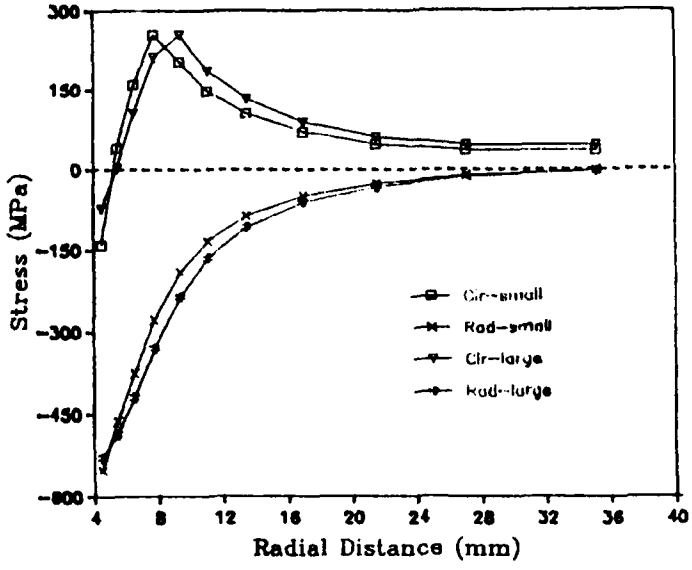

FIG.9.26 5% COLD-EXPANSION OF A HOLE IN A LARGE ALUMINIUM ALLOY PLATE - EFFECT OF DISPLACEMENT THEORY (SMALL VS LARGE)

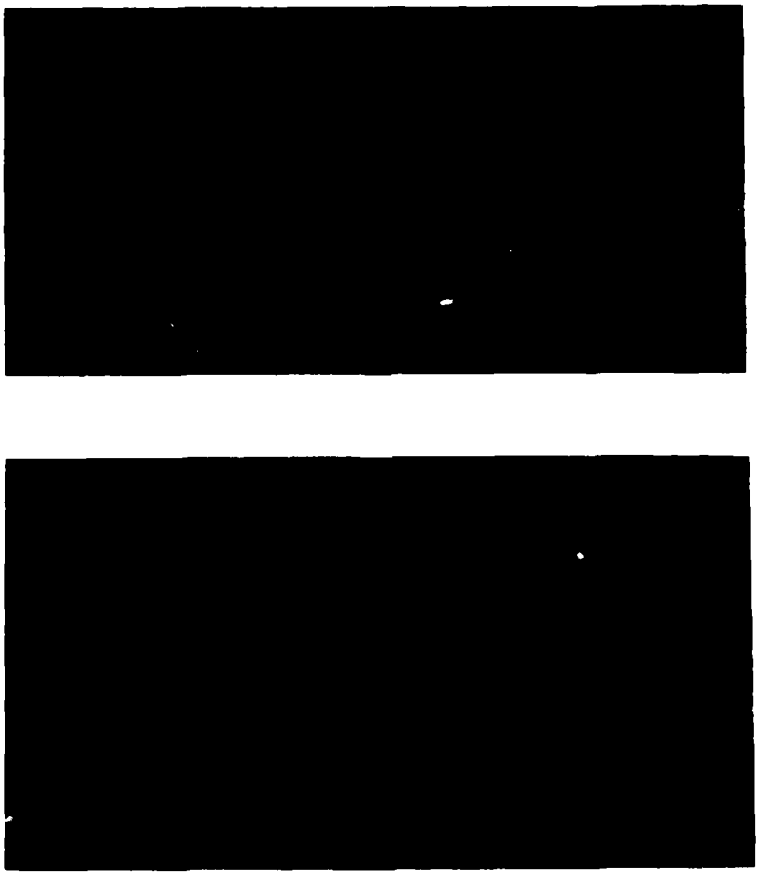

(a)

(b)

FIG.9.27 REPLICAS OF CRACK TIP REGION DISPLACEMENT DISTRIBUTIONS (a) JUST BEFORE (b) JUST AFTER INITIAL J-INTEGRAL CRACK EXTENSION (2024-T351 ALUMINIUM ALLOY)

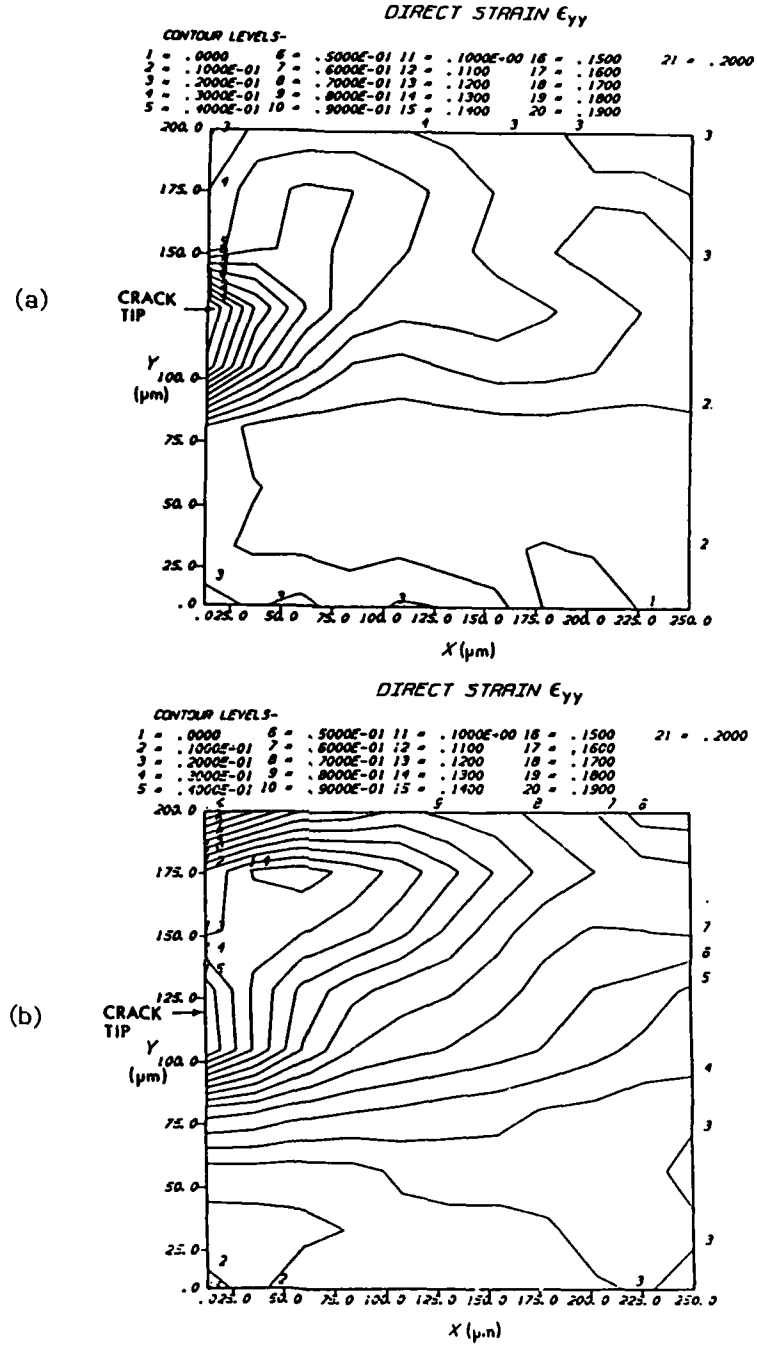

(a) ΔK = 20 MPa$\sqrt{m}$, R = 0.5

(b) ΔK = 25 MPa$\sqrt{m}$, R = 0.5

FIG.9.28 COMPUTER GENERATED STRAIN CONTOUR PLOTS FROM MICROGRID DISPLACEMENT MEASUREMENTS FOR TWO LOADING CONDITIONS

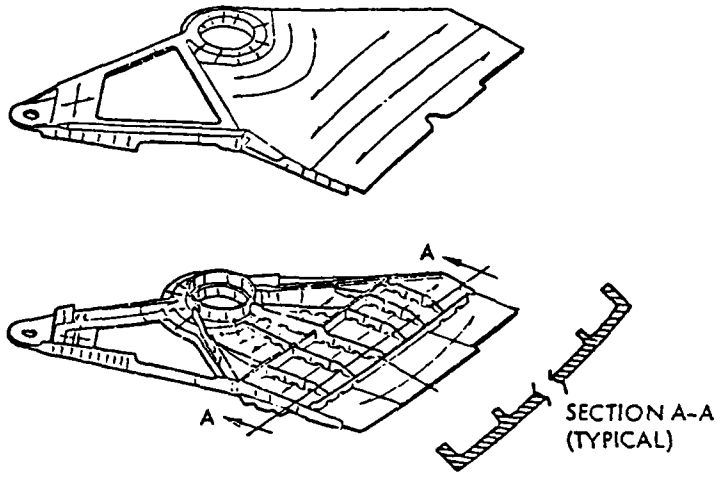

FIG.9.29 D6ac STEEL WING PIVOT FITTINGS OF F-111 AIRCRAFT - UPPER AND LOWER SURFACES

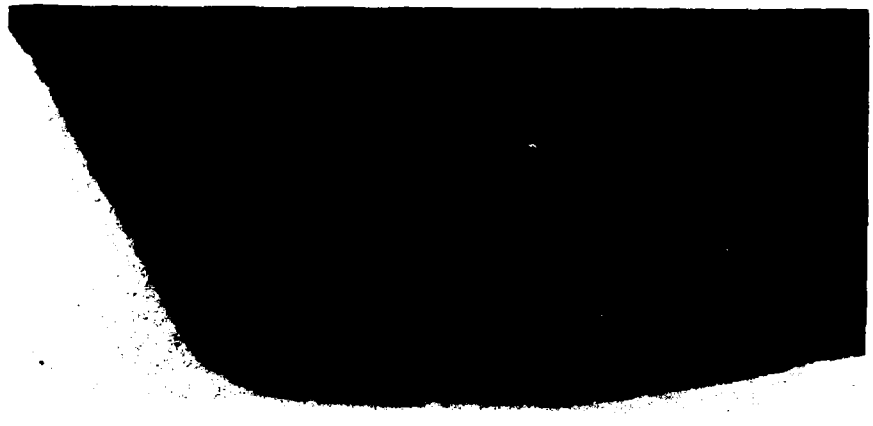

(a) Fracture surface

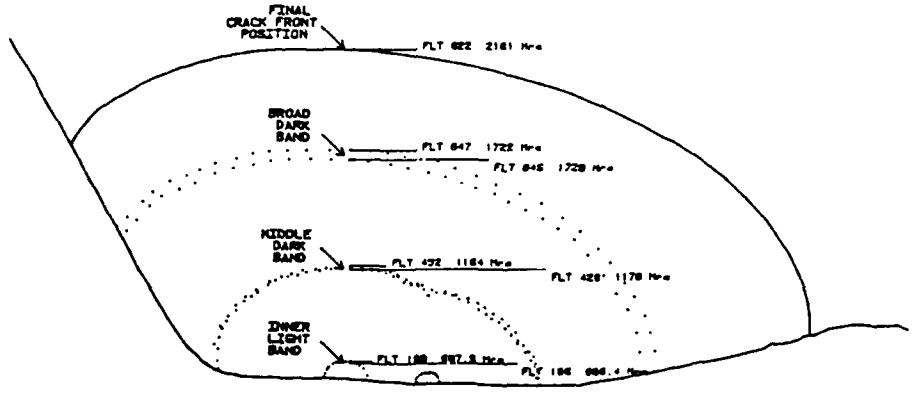

(b) Quantitative fractographic allocation of fracture surface markings to events

FIG.9.30 CRITICAL CRACK FROM F-111 WING PIVOT FITTING WHICH FAILED DURING COLD PROOF LOAD TESTING

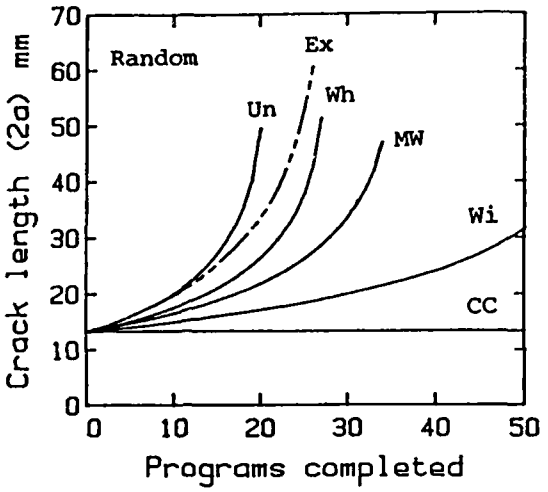

FIG.9.31 COMPARISON OF PREDICTED AND ACTUAL FATIGUE CRACK GROWTH

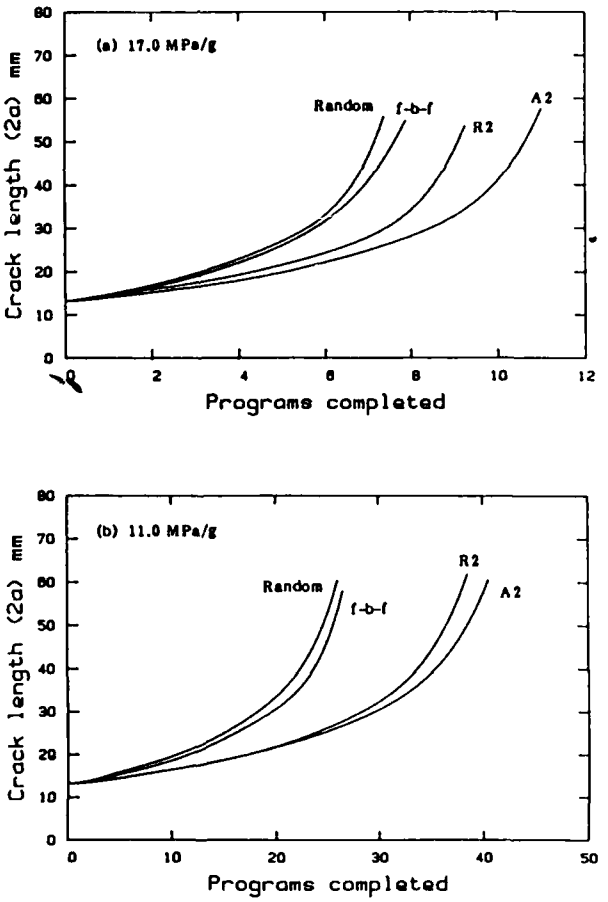

FIG.9.32 FATIGUE CRACK GROWTH IN CENTRE-CRACKED SPECIMENS AT TWO STRESS LEVELS FOR FOUR SEQUENCES ALL HAVING IDENTICAL RANGE-PAIR-COUNTS

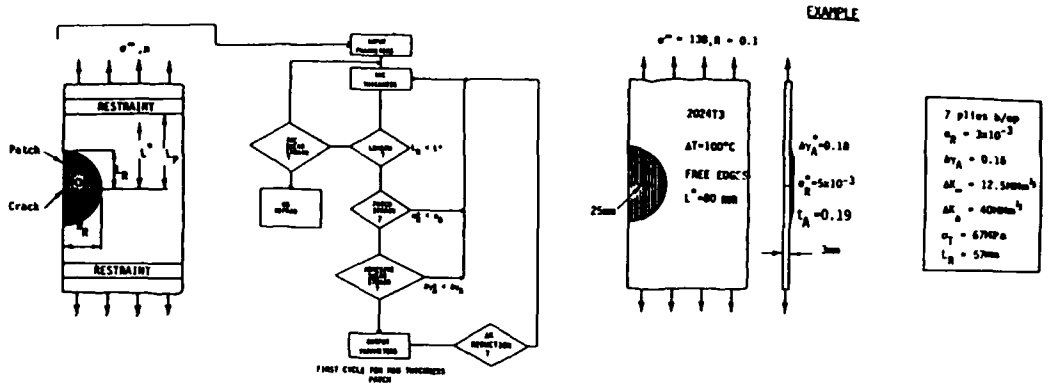

FIG.9.33 CRACK PATCHING SCHEMATIC SHOWING SIMPLIFIED FLOW CHART FOR PATCH ANALYSIS AND AN EXAMPLE RELATED TO EXPERIMENTAL STUDIES

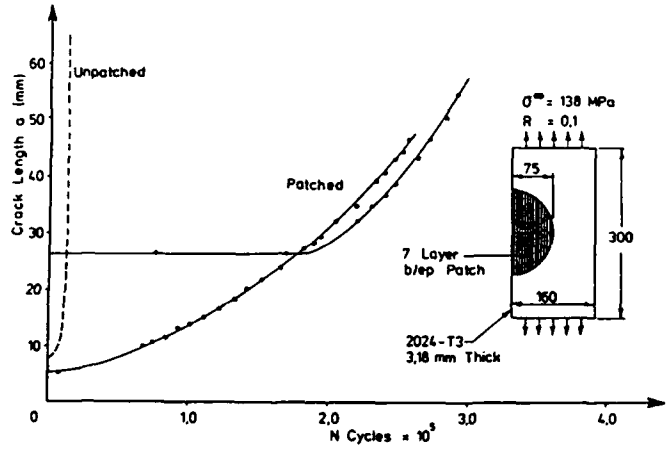

FIG.9.34 CRACK GROWTH CURVES FOR PATCHED (AF 126 ADHESIVE) AND UNPATCHED SPECIMENS

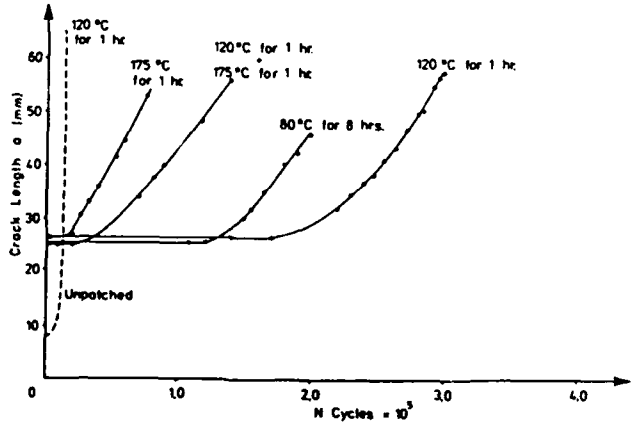

FIG.9.35 CRACK GROWTH CURVES FOR SPECIMENS SUBJECTED TO DIFFERING HEAT-TREATMENT DURING PATCH APPLICATION

FIG.9.36 F-111 WING STATIC TEST RIG

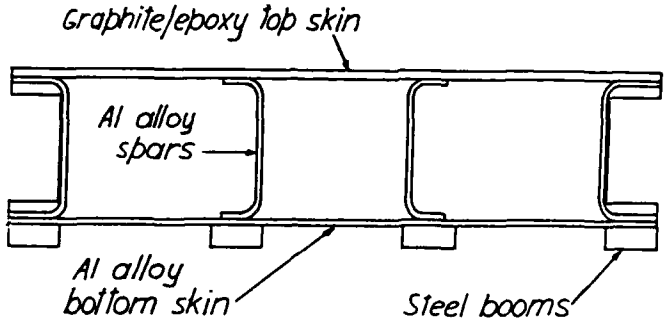

FIG.9.37 CROSS-SECTION OF GRAPHITE/EPOXY - ALUMINIUM ALLOY BOX-BEAM

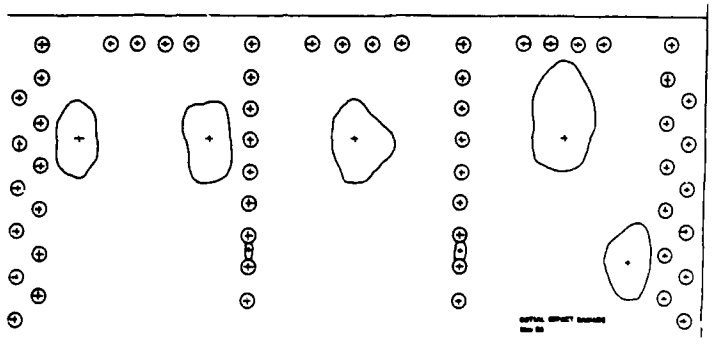

FIG.9.38 BOX-BEAM SPECIMEN - INPACT DAMAGE MAP

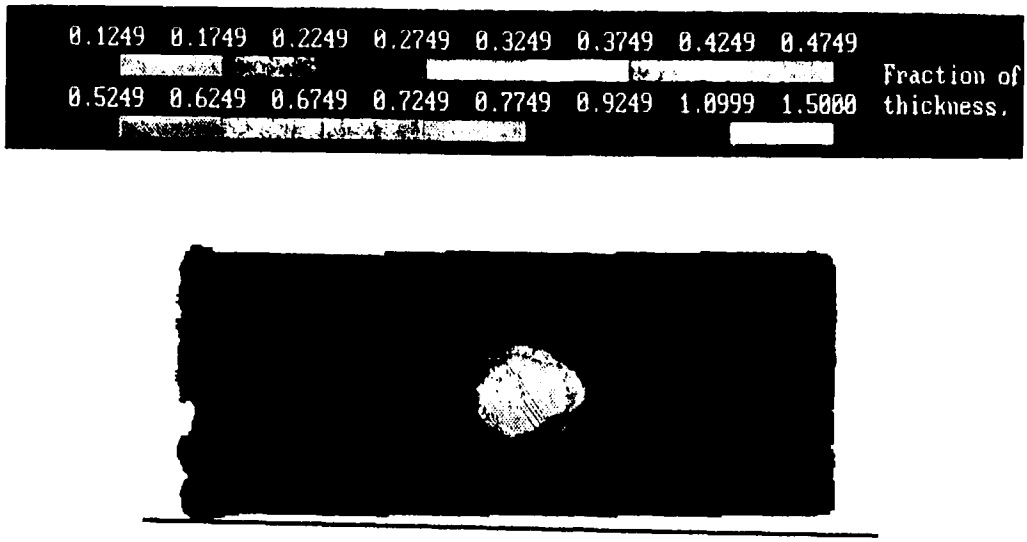

FIG.9.39 DEPTH C-SCAN OF AN IMPACT DAMAGED CARBON FIBRE COMPOSITE LAMINATE

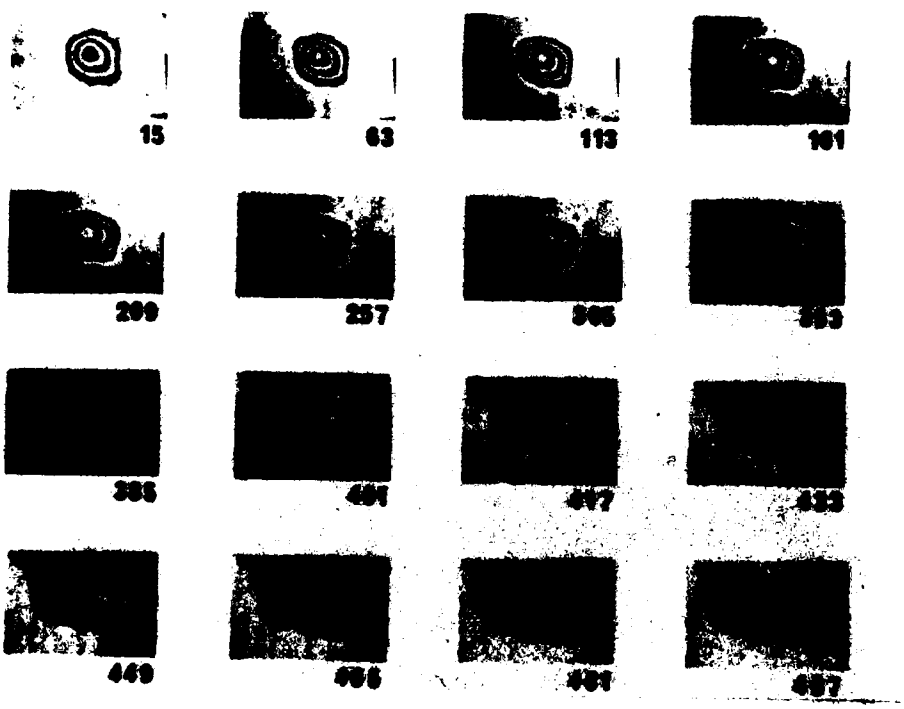

FIG.9.40 SHADOW MOIRE FRINGES INDICATING GROWTH IN INITIAL IMPACT DAMAGED AREA WITH FATIGUE LOADING BLOCKS - MAJOR GROWTH DIRECTION IS NORMAL TO LOADING DIRECTION/0^{o} FIBRE DIRECTION

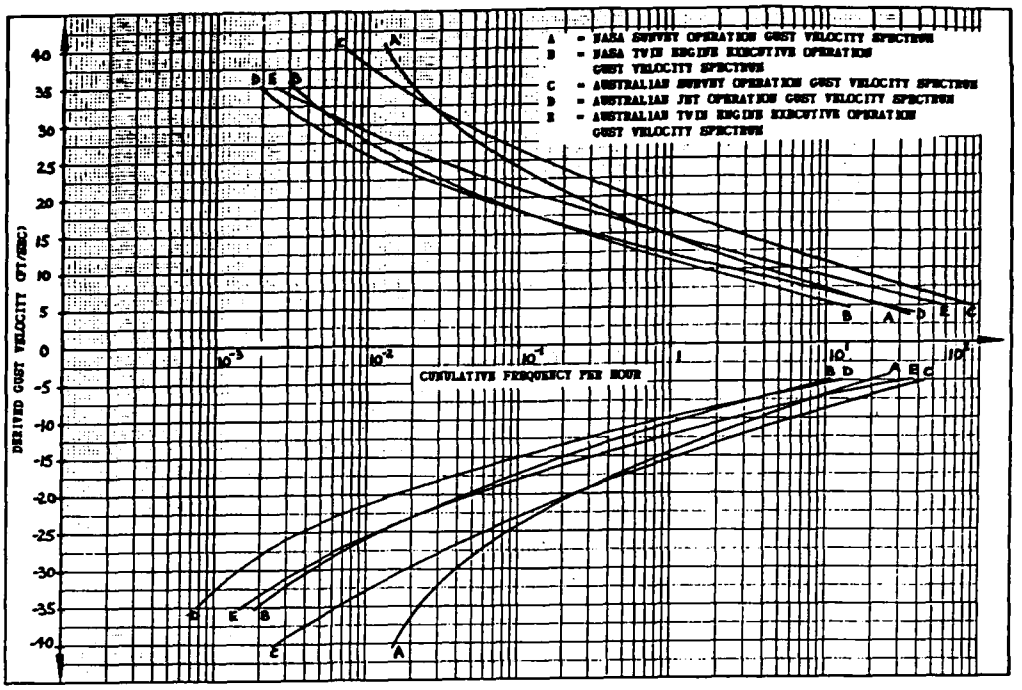

FIG.9.41 FITTED GUST SPECTRA POLYNOMIALS FOR AUSTRALIAN AND NASA GUST DATA

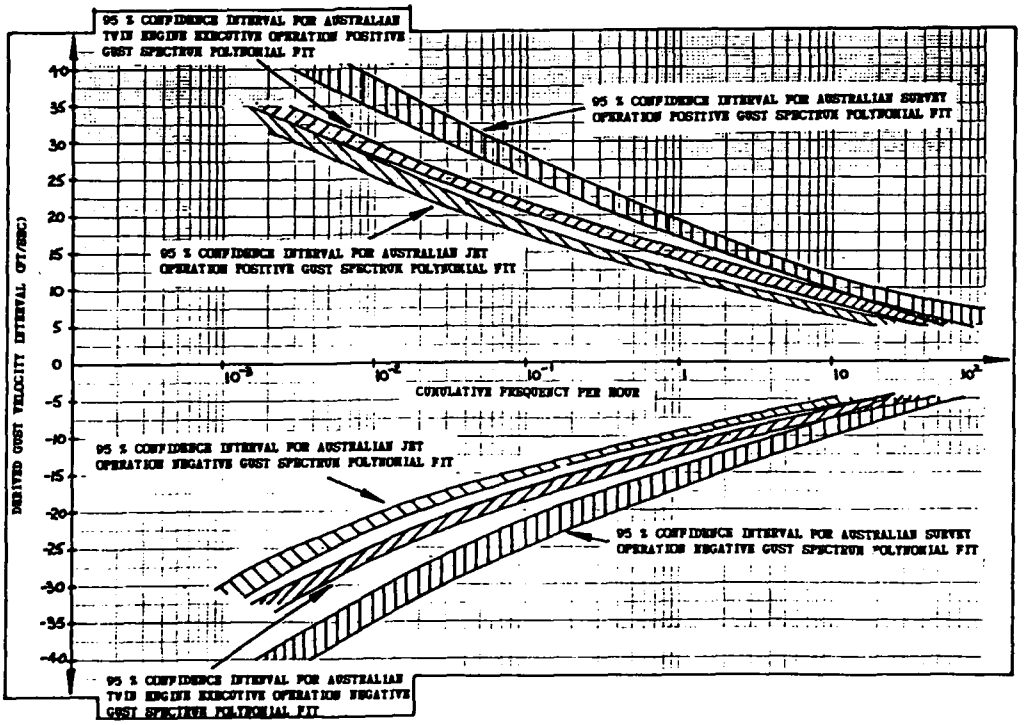

FIG.9.42 95% CONFIDENCE INTERVALS FOR FITTED AUSTRALIAN GUST SPECTRA POLYNOMIALS

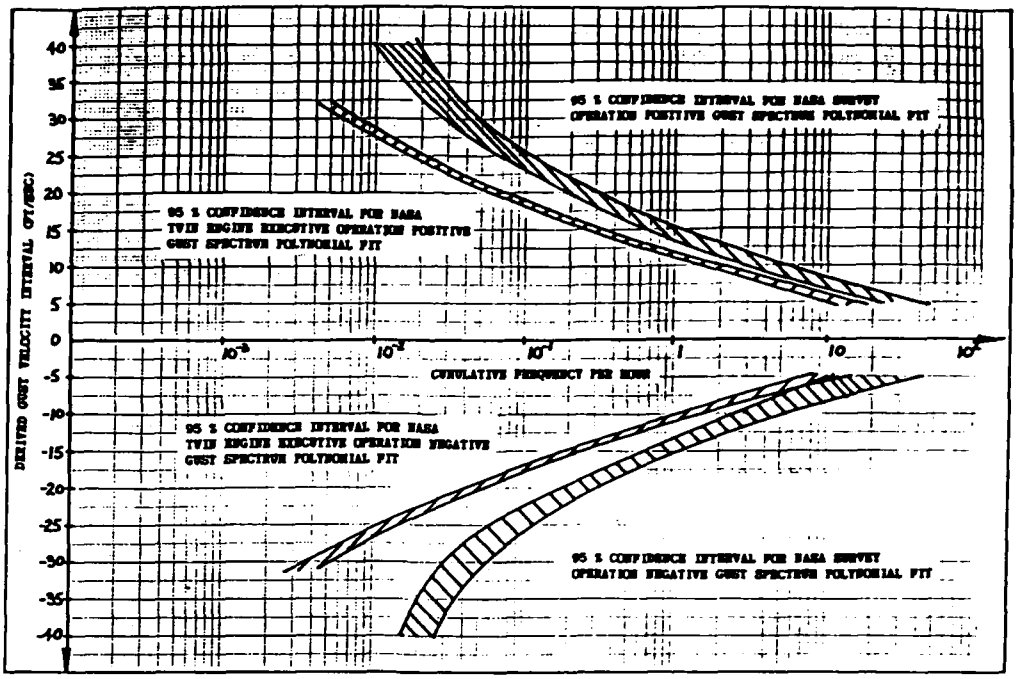

FIG.9.43 95% CONFIDENCE INTERVALS FOR FITTED NASA GUST SPECTRA POLYNOMIALS

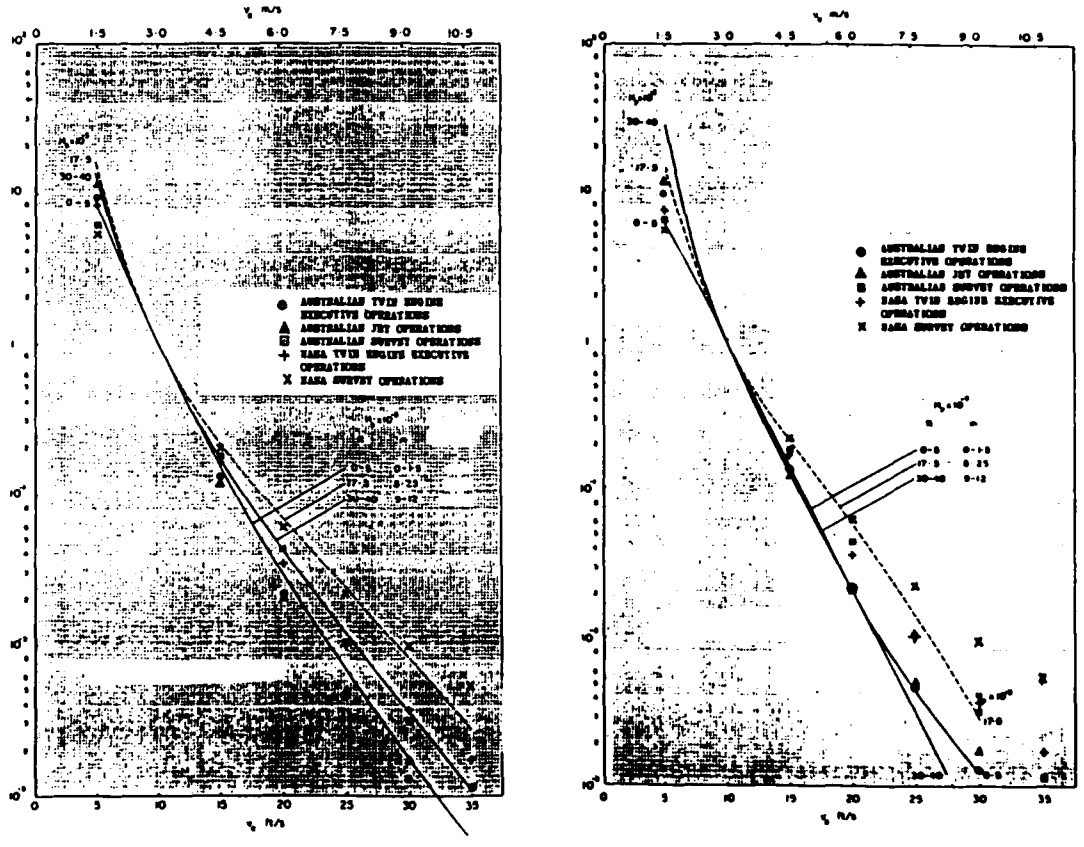

(a) without cloud radar (b) with cloud radar

FIG. 9.44 VARIATION OF RELATIVE GUST FREQUENCY WITH GUST VELOCITY - COMPARISON OF ESDU, NASA AND AUSTRALIAN DATA

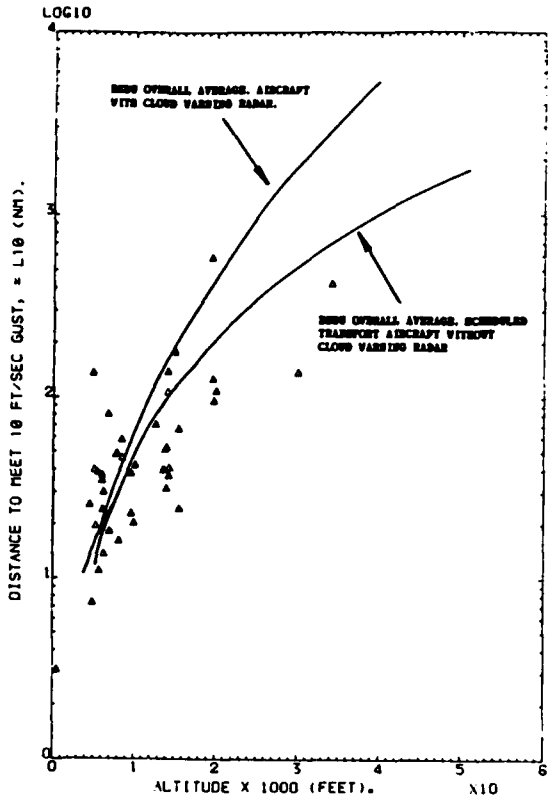

FIG.9.45 VARIATION OF ABSOLUTE GUST FREQUENCY WITH ALTITUDE - FROM THE AUSTRALIAN FLIGHT LOADS ANALYSIS PROGRAMME

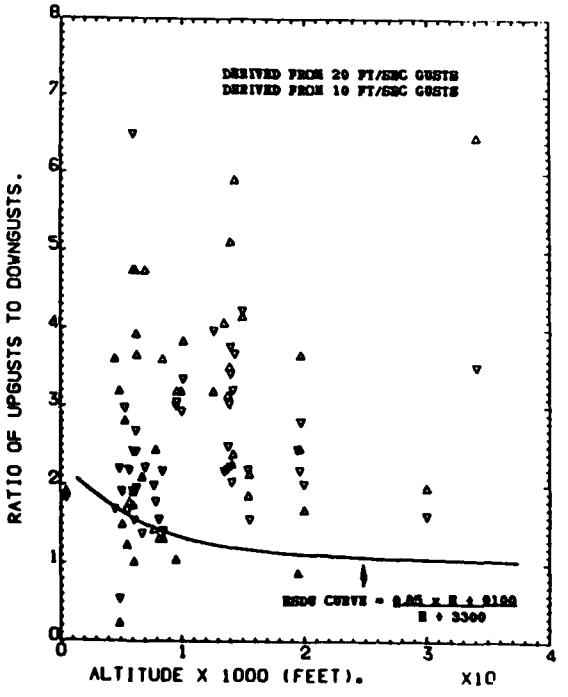

FIG.9.46 VARIATION OF RATIO OF UPGUSTS TO DOWNGUSTS WITH ALTITUDE - FROM THE AUSTRALIAN FLIGHT LOADS ANALYSIS PROGRAMME

DISTRIBUTION

AUSTRALIA

Department of Defence

Defence Central

Chief Defence Scientist
Deputy Chief Defence Scientist)
Superintendent, Science and Program Administration) shared copy
Controller, External Relations, Projects and)
Analytical Studies)
Director, Departmental Publications
Counsellor, Defence Science (London) (Doc Data Sheet Only)
Counsellor, Defence Science (Washington) (Doc Data Sheet Only)
SA to the Thailand Military R and D Centre (Doc Dats Sheet Only)
SA to the DRC (Kuala Lumpur) (Doc Data Sheet Only)
Defence Central Library
Document Exchange Centre, DISB (18 copies)
Joint Intelligence Organisation
Librarian H Block, Victoria Barracks, Melbourne
Director General - Army Development (NSO) (4 copies)
Defence Industry and Material Policy, FAS

Aeronautical Research Laboratories

Director
Library
Divisional File - Structures
J.Y. Mann
B.C. Hoskin
D.G. Ford
C.K. Rider
J.L. Kepert
J.M. Finney
J.G. Sparrow
R. Jones
D.J. Sherman
D. Saunders
J.M. Grandage
R.G. Parker
K.C. Watters
P.W. Beaver
L.R. Gratzer
R.P. Carey
T.J. van Blaricum
G.S. Jost (for ICAF Distribution (225 copies)
C.K. Rider (for TTCP Distribution (5 copies)
Superintendent - Aircraft Materials
A.A. Baker
N.E. Ryan
G. Clark
B.J. Wicks
N.T. Goldsmith
Superintendent - Aerodynamics

Superintendent - Aero Propulsion
Superintendent - Systems
Principal Engineer
Author: G.S. Jost

Materials Research Laboratories
Director/Library

Defence Research Centre
Library

RAN Research Laboratory
Library

Navy Office
Navy Scientific Adviser
Director of Naval Aircraft Engineering

Army Office
Scientific Adviser - Army
Engineering Development Establishment, Library
Royal Military College Library

Air Force Office
Air Force Scientific Adviser
Aircraft Research and Development Unit
Scientific Flight Group
Library
Technical Division Library
Director General Aircraft Engineering - Air Force
HQ Support Command (SLENGO)
RAAF College, Point Cook

Government Aircraft Factories
Manager
Library
L.T. Tuller

Department of Aviation
Library
Flight Standards Division
C. Torkington
R.B. Doublas
C. Stefoulis

Department of Industry, Technology and Commerce
Library

Statutory and State Authorities and Industry
Australian Airlines, Library
Qantas Airways Limited
Ansett Airlines of Australia
Library
J.H. Bibo

BHP, Melbourne Research Laboratories
Hawker de Havilland Aust Pty Ltd, Bankstown
Library
I.D. McArthur
Hawker de Havilland Aust Pty Ltd, Victoria
Library
P.J. Foden

Universities and Colleges

Adelaide
Barr Smith Library
Flinders
Library
La Trobe
Library
Melbourne
Engineering Library
Dr J.F. Williams
Monash
Hargrave Library
Prof I.J. Polmear, Materials Engineering
Newcastle
Library
New England
Library
Sydney
Engineering Library
Dr G.P. Steven
NSW
Physical Sciences Library
Prof R.A.A. Bryant, Mechanical Engineering
Queensland
Library
Tasmania
Engineering Library
Western Australia
Library

NEW ZEALAND

Defence Scientific Establishment, Library
RNZAF, Vice Consul (Defence Liaison)
Transport Ministry, Airworthiness Branch, Library

Universities

Canterbury
Library
Auckland
Library
Wellington
Library

SPARES (20 copies)
TOTAL (365 copies)

Department of Defence

DOCUMENT CONTROL DATA

1.a. AR No	1.b. Establishment No	2. Document Date	3. Task No
AR-004-521	ARL-STRUC-TM-457	April 1987	DEF 89/501

4. Title	5. Security	6. No Pages	7. No Refs
A REVIEW OF AUSTRALIAN INVESTIGATIONS ON AERONAUTICAL FATIGUE DURING THE PERIOD APRIL 1985 TO MARCH 1987.	a. document: UNCLASSIFIED b. title: U c. abstract: U	56	64

8. Author(s)	9. Downgrading Instructions
G.S. JOST	

10. Corporate Author and Address	11. Authority (as appropriate) a.Sponsor b.Security c.Downgrading d.Approval
Aeronautical Research Laboratories P.O. Box 4331, MELBOURNE, VIC. 3001	

12. Secondary Distribution (of this document)

Approved for Public Release.

Overseas enquirers outside stated limitations should be referred through ASDIS, Defence Information Services Branch, Department of Defence, Campbell Park, CANBERRA ACT 2601

13.a. This document may be ANNOUNCED in catalogues and awareness services available to ...

No limitations.

13.b. Citation for other purposes (ie casual announcement) may be (select) unrestricted(or) as for 13 a.

14. Descriptions	15. COSATI Group
Aircraft Fatigue (materials) Aircraft Structures	0051C 0071L

16. Abstract

This document was prepared for presentation to the 20th Conference of the International Committee on Aeronautical Fatigue scheduled to be held at Ottawa, Canada, on June 8 and 9, 1987. A review is given of Australian aircraft fatigue research and associated activities. The major topics discussed include fatigue in both civil and military aircraft structures, fatigue damage repair and analysis and fatigue life monitoring and assessment.

PF 65

This paper is to be used to record information which is required by the Establishment for its own use but which will not be added to the DISTIS data base unless specifically requested.

16. Abstract (contd)

17. Imprint

Aeronautical Research Laboratories, Melbourne

18. Document Series and Number	19. Cost Code	20. Type of Report and Period Covered
Structures Technical Memorandum	24 1100	

21. Computer Programs Used

22. Establishment File Ref(s)

M3/48

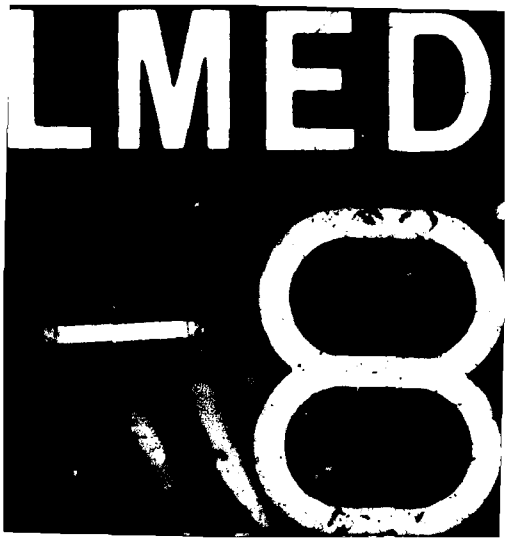
LMED
8